Table 4. Correlations between changes in basic activity of daily living (ADL) score during 2-year study period and anthropometric measurements during 2-year study period

	Change of ADL score during 2-year follow-up		
Changes in levels during 2-year period	All participants (*n* 543)	Excluded basic ADL score of 0 at baseline (*n* 468)	Basic ADL score of 12 or higher† at baseline (*n* 291)
BMI (kg/m^2)			
Crude	0·123*	0·117	0·134
Adjusted‡	0·149*	0·137*	0·191**
Mid-arm circumference (cm)			
Crude	0·157**	0·169**	0·099
Adjusted‡	0·152**	0·158**	0·169**

Mean values were significantly different: *$P<0·05$, **$P<0·01$.
† The 50th percentile of basic ADL scores at baseline was 12 in the present study.
‡ Adjusted for age and sex.

measurements and ADL function decline nor between basal poor ADL performance and a decrease in anthropometric parameters.

Previous prospective cohort studies emphasised that weight loss is a risk factor for the functional decline[8–12]. However, no studies allow the evaluation of causal relationships between weight loss and the functional decline. In the present study, we showed that physical functional change was well correlated with change in anthropometric parameters. In addition, logistic regression models demonstrated that the decline in anthropometric parameters was a predictor of the decline in ADL performance, and that, conversely, the decline in ADL performance was also a predictor of anthropometrics decline. These results may indicate that these factors, anthropometric parameters and ADL status, influence each other and decline simultaneously. BMI and AC are parameters of nutritional status in older adults[26,27]. Therefore, the results may indicate that nutritional status and ADL performance were well correlated and changed simultaneously through causal and consequential relationships. Theoretically, inadequate intake of nutrients, one of the manifestations of undernutrition, which can lead to loss of muscle protein as well as body mass, may explain the association between weight loss and decline in physical function. In contrast, physical functional decline may be a cause of weight loss through difficulties in eating, provisioning and cooking, which can be reflected by a decline in the food-related items of the ADL.

It is possible that there are third factors that might produce the association between the loss of anthropometric parameters and the decline in ADL performance during the follow-up period. The occurrence of new diseases or poor control of chronic disease during the follow-up period might be a candidate for the third factor. However, the association persisted even after adjusting for hospitalisation for acute illness during the study period, which suggests that poor health outcomes leading to hospitalisation did not contribute to these relationships.

The present study has several limitations. The results of the present study cannot be transferred to non-frail-independent

Table 5. Logistic regression analysis to identify independent predictors of declining basic activity of daily living (ADL) score, declining BMI and arm circumference
(OR values with 95% CI)

				Multivariate					
	Unadjusted			Model 1			Model 2		
	OR	95% CI	*P*	OR	95% CI	*P*	OR	95% CI	*P*
Basic ADL decline *v.* improve/stable*									
Change in BMI levels during 2-year period									
Increase or stable	1·00	Reference		1·00	Reference		1·00	Reference	
Decline (<1·0 kg/m^2)	1·09	0·50, 2·39	0·833	0·90	0·31, 2·09	0·810	0·89	0·30, 2·58	0·822
Decline (≥ 1·0 kg/m^2)	3·86	1·96, 7·59	<0·001	3·64	1·73, 7·65	0·001	4·69	1·89, 11·67	0·001
Change in AC levels during 2-year period									
Increase or stable	1·00	Reference		1·00	Reference		1·00	Reference	
Decline (≤ 0·5 cm)	1·55	0·66, 3·65	0·319	1·52	0·60, 3·83	0·373	1·00	0·31, 3·25	0·998
Decline (0·6–1·5 cm)	1·77	0·91, 3·45	0·092	2·54	1·20, 5·38	0·015	2·80	1·02, 7·69	0·045
Decline (≥ 1·6 cm)	2·75	1·63, 4·64	<0·001	3·45	1·88, 6·35	<0·001	3·18	1·40, 7·20	0·006
Loss of BMI levels *v.* increase/stable†									
Change in basic ADL score during 2-year period									
Improved or stable	1·00	Reference		1·00	Reference		1·00	Reference	
Decline (1 point)	1·95	0·87, 4·42	0·107	1·94	0·77, 4·84	0·158	2·67	0·93, 7·70	0·069
Decline (≥ 2 points)	2·33	1·20, 4·55	0·013	3·28	1·50, 7·17	0·003	3·28	1·32, 8·16	0·011
Loss of AC levels *v.* increase/stable‡									
Change in basic ADL score during 2-year period									
Improved or stable	1·00	Reference		1·00	Reference		1·00	Reference	
Decline (1 point)	1·40	0·74, 2·66	0·307	1·17	0·55, 2·49	0·678	1·01	0·40, 2·58	0·981
Decline (> 2 points)	2·90	1·72, 4·89	<0·001	3·62	1·95, 6·73	<0·001	2·94	1·35, 6·38	0·007

The 50th percentile of basic ADL scores at baseline was 12 in the present study.
* Multivariate analysis includes sex, age, presence or absence of hypertension and neurodegenerative disease, hospitalisation and fall experience during the 2-year period and the score of basic ADL at baseline. BMI: *n* 135. mid-arm circumference (AC): *n* 416. Model 2 participants that had a basic ADL score of 12 or higher at baseline. BMI: *n* 182. AC: *n* 245.
† Multivariate analysis includes sex, age, living alone, regular medical checkups, cerebrovascular disease, hospitalisation during the 2-year period and the score of BMI at baseline. Participants had a basic ADL score of 2 or higher at baseline (*n* 225). Model 2 participants that had a basic ADL score of 12 or higher at baseline. *n* 172.
‡ Multivariate analysis includes sex, age, living alone, regular medical checkups, cerebrovascular disease, hospitalisation during the 2-year period and the score of AC at baseline. Participants had a basic ADL score of 2 or higher at baseline. *n* 342. Model 2 participants that had a basic ADL score of 12 or higher at baseline (*n* 228).

NS British Journal of Nutrition

older individuals, since there are many differences between the participants in Nagoya Longitudinal Study for Frail Elderly and standard non-frail older people, including differences in ADL levels and comorbidity. There was a possibility that the presence of lower BMI levels and fewer obese individuals in our cohort may have affected the present results. In addition, these findings may not be generalisable to other populations, given that they may have been influenced by cultural differences, health practices and a variety of social and economic factors. The mechanisms underlying the association between the decline in BMI/AC levels and declining ADL score during the 2-year follow-up period are unclear in the present study. Future study is needed to examine whether the ADL scores and anthropometric measurements of these frail elderly with functional limitations in the community decrease concurrently.

The present study showed that anthropometric measurements at baseline were not a predictor of physical function decline during a 2-year follow-up in community-dwelling elderly. An association was found between negative changes in anthropometric measurements during the follow-up period and the decline in ADL function.

Acknowledgements

The authors wish to thank all the patients, caregivers and the many nurses participating in the study, and the Nagoya City Health Care Service Foundation for Older People for their vigorous cooperation. The present study was supported by a Grant-in-Aid for the Comprehensive Research on Aging and Health from the Ministry of Health, Labor and Welfare of Japan, and a grant from Mitsui Sumitomo Insurance Welfare Foundation. The authors have no conflicts of interest with the manufactures of any drug evaluated in the present paper. S. I. contributed to the analysis of data and the writing of the manuscript. H. E. contributed to the analysis and interpretation data. Y. H. contributed to conduct of study and interpretation of data. M. I. contributed to analysis and interpretation of data. J. H. contributed to acquisition of data. A. I. contributed to the providing of significant advice. M. K. contributed to the study concept and design, the interpretation of data, and was performing quality control of the present study.

References

1. Stuck AE, Walthert JM, Nikolaus T, *et al.* (1999) Risk factors for functional status decline in community-living elderly people: a systematic literature review. *Soc Sci Med* **48**, 445–469.
2. Topinková E (2008) Aging, disability and frailty. *Ann Nutr Metab* **52**, Suppl. 1, 6–11.
3. Zoico E, Di Francesco V, Guralink JM, *et al.* (2004) Physical disability and muscular strength in relation to obesity and different body composition indexes in a sample of healthy elderly women. *Int J Obes Relat Metab Disord* **28**, 234–241.
4. Larrieu S, Pérès K, Letenneur L, *et al.* (2004) Relationship between body mass index and different domains of disability in older persons: the 3C study. *Int J Obes Relat Metab Disord* **28**, 1555–1560.
5. Friedmann JM, Elasy T & Jensen GL (2001) The relationship between body mass index and self-reported functional limitation among older adults: a gender difference. *J Am Geriatr Soc* **49**, 398–403.
6. Chen H & Guo X (2008) Obesity and functional disability in elderly Americans. *J Am Geriatr Soc* **56**, 689–694.
7. Romagnoni F, Zuliani G, Bollini C, *et al.* (1999) Disability is associated with malnutrition in institutionalized elderly people. The I.R.A. Study. Istituto di Riposo per Anziani. *Aging (Milano)* **11**, 194–199.
8. Launer LJ, Harris T, Rumpel C, *et al.* (1994) Body mass index, weight change, and risk of mobility disability in middle-aged and older women. The epidemiologic follow-up study of NHANES I. *JAMA* **271**, 1093–1098.
9. Tully CL & Snowdon DA (1995) Weight change and physical function in older women: findings from the Nun Study. *J Am Geriatr Soc* **43**, 1394–1397.
10. Al Snih S, Raji MA, Markides KS, *et al.* (2005) Weight change and lower body disability in older Mexican Americans. *J Am Geriatr Soc* **53**, 1730–1737.
11. Ritchie CS, Locher JL, Roth DL, *et al.* (2008) Unintentional weight loss predicts decline in activities of daily living function and life-space mobility over 4 years among community-dwelling older adults. *J Gerontol A Biol Sci Med Sci* **63**, 67–75.
12. Jensen GL & Friedmann JM (2002) Obesity is associated with functional decline in community-dwelling rural older persons. *J Am Geriatr Soc* **50**, 918–923.
13. Mahoney F & Barthel DW (1965) Functional evaluation: The Barthel Index. *Md State Med J* **14**, 61–65.
14. Collin C, Wade DT, Davies S, *et al.* (1998) The Barthel ADL Index: a reliability study. *Int Disabil Stud* **10**, 61–63.
15. Izawa S, Enoki H, Hirakawa Y, *et al.* (2007) Lack of body weight measurement is associated with mortality and hospitalization in community-dwelling frail elderly. *Clin Nutr* **26**, 764–770.
16. Enoki H, Kuzuya M, Masuda Y, *et al.* (2007) Anthropometric measurements of mid-upper arm as a mortality predictor for community-dwelling Japanese elderly: the Nagoya Longitudinal Study of Frail Elderly (NLS-FE). *Clin Nutr* **26**, 597–604.
17. Kuzuya M, Masuda Y, Hirakawa Y, *et al.* (2006) Underuse of medications for chronic diseases in the oldest of community-dwelling older frail Japanese. *J Am Geriatr Soc* **54**, 598–605.
18. Kuzuya M, Masuda Y, Hirakawa Y, *et al.* (2006) Day care service use is associated with lower mortality in community-dwelling frail older people. *J Am Geriatr Soc* **9**, 1364–1371.
19. Campbell JC & Ikegami N (2000) Long-term care insurance comes to Japan. *Health Aff (Millwood)* **19**, 26–39.
20. Tsutsui T & Muramatsu N (2005) Care-needs cerfication in the long-term care insurance system of Japan. *J Am Geriatr Soc* **53**, 522–527.
21. Arai Y, Kudo K, Hosokawa T, *et al.* (1997) Reliability and validity of the Japanese version of the Zarit Caregiver Burden interview. *Psychiatry Clin Neurosci* **51**, 281–287.
22. Charlson ME, Pompei P, Ales KL, *et al.* (1987) A new method of classifying prognostic comorbidity in longitudinal studies: development and validation. *J Chronic Dis* **40**, 373–383.
23. World Health Organization (1986) Use and interpretation of anthropometric indicators of nutritional status: report of a WHO working group. *Bull World Health Organ* **64**, 929–941.
24. Heymsfield SB, McManus C, Smith J, *et al.* (1982) Anthropometric measurement of muscle mass: revised equations for calculating bone-free arm muscle area. *Am J Clin Nutr* **36**, 680–690.
25. Japanese Anthropometric Reference Data (2002) JARD 2001, Japanese Anthropometric Reference Data (in Japanese). *Jpn J Nutr Assess* **19**, Suppl., 45–81.
26. Gariballa S & Forster S (2007) Malnutrition is an independent predictor of 1-year mortality following acute illness. *Br J Nutr* **98**, 332–336.
27. Izawa S, Kuzuya M, Okada K, *et al.* (2006) The nutritional status of frail elderly with care needs according to the mini-nutritional assessment. *Clin Nutr* **25**, 962–967.

Mechanism of Diastolic Stiffening of the Failing Myocardium and Its Prevention by Angiotensin Receptor and Calcium Channel Blockers

Xian Wu Cheng, MD, PhD,† Kenji Okumura, MD, PhD,* Masafumi Kuzuya, MD, PhD,‡ Zhehu Jin, MD, PhD,†‡ Kohzo Nagata, MD, PhD,§ Koji Obata, PhD,¶ Aiko Inoue, MS,‡ Akihiro Hirashiki, MD, PhD,* Kyosuke Takeshita, MD, PhD,* Kazumasa Unno, MD,* Ken Harada, MD,* Guo-Ping Shi, DSc,‖ Mitsuhiro Yokota, MD, PhD,** and Toyoaki Murohara, MD, PhD**

Objective: To investigate the mechanism responsible for the increased cardiac stiffness associated with hypertensive heart failure in Dahl salt-sensitive (DS) rats and the effects of treatment with the combination of a calcium channel blocker [azelnidipine (AZE)] and angiotensin II type 1 receptor blocker [olmesartan (OLM)].

Methods: DS rats fed a high-salt diet from 7 weeks of age were treated (or not) from 12 to 19 weeks of age with the vasodilator hydralazine, OLM plus AZE, or the reduced nicotinamide adenine dinucleotide phosphate (NADPH) oxidase inhibitor apocynin. Rats fed a low-salt diet served as controls.

Results: Treatment with OLM plus AZE attenuated changes in the expression of collagen isoforms and a decrease in the ratio of elastin to collagen in the left ventricle and prevented the increase in myocardial stiffness and diastolic dysfunction in DS rats in a manner independent of the hypotensive effect of these drugs. Such treatment also inhibited the expression and activation of elastolytic proteases (including cathepsins S and K and metalloproteinases-2, -9, and -12), NADPH oxidase–dependent superoxide production, and inflammatory changes in the failing myocardium. All these effects were mimicked by treatment with apocynin.

Conclusions: The changes in collagen isoform expression and the decrease in the elastin to collagen ratio in the failing myocardium likely account for the increase in diastolic stiffness in this model of hypertensive heart failure. Administration of angiotensin receptor and calcium channel blockers prevented these changes in a manner independent of the hypotensive effect of these drugs by inhibiting the increase in elastolytic activity induced by activation of NADPH oxidase.

Key Words: cardiac stiffness, heart failure, collagen, elastin, oxidative stress, elastase

(*J Cardiovasc Pharmacol*™ 2009;54:47–56)

INTRODUCTION

Increased stiffness of the left ventricle (LV) during diastole is the earliest manifestation of hypertension-induced LV dysfunction and is often the main functional deficit of the heart associated with hypertension, given that many hypertensive patients who develop heart failure (HF) have a normal LV ejection fraction.[1,2] This increased LV stiffness is associated with marked changes in the extracellular matrix (ECM). Experimental and clinical studies have thus shown that hypertensive heart disease is accompanied by increased collagen expression, collagen density, and fibrillar collagen content and by altered fibrillar collagen geometry.[2–4] However, the specific molecular and biochemical mechanisms that underlie this ECM remodeling and the increase in LV stiffness in animals or patients with hypertensive heart disease have remained unclear. Two of the major determinants of ECM homeostasis are the rate and extent of ECM degradation. ECM degradation is mediated by cardiac cell–derived proteases such as matrix metalloproteinases (MMPs) and cysteine proteases.[1,3–5] Extensive evidence supports a role for MMPs in cardiac ECM remodeling,[1,5] and cathepsins, which are lysosomal cysteine proteases, show pronounced elastolytic and collagenolytic activities both in vitro and in vivo and are overexpressed in the failing myocardium of animals or patients

Received for publication February 6, 2009; accepted April 22, 2009.

From the *Department of Cardiology, Nagoya University Graduate School of Medicine, Nagoya, Japan; †Department of Cardiology, Yanbian University Hospital, Yanji, China; ‡Department of Geriatrics, Nagoya University Graduate School of Medicine, Nagoya, Japan; §Department of Medical Technology, Nagoya University School of Health Sciences, Nagoya, Japan; ¶Department of Pharmacology, Aichi Gakuin University School of Dentistry, Nagoya, Japan; ‖Department of Cardiovascular Medicine, Brigham and Women's Hospital, Harvard Medical School, Boston, MA; and **Department of Genome Science, Aichi Gakuin University School of Dentistry, Nagoya, Japan.

Supported in part by grants from the Ministry of Education, Culture, Sports, Science, and Technology of Japan (nos. 17590719 and 19590812 to X.W.C.) and from the Japan Heart Foundation (no. 26-7508 to X.W.C.); by a Japan Heart Foundation/Novartis Research Award on Molecular and Cellular Cardiology (no. 26-7523 to X.W.C); and by a grant from the Takeda Science Foundation (no. 26-7527 to X.W.C).

The authors report no conflicts of interest.

Reprints: Xian Wu Cheng, MD, PhD, Department of Cardiology, Nagoya University School of Medicine, 65 Tsuruma-cho, Showa-ku, Nagoya 466-8550, Japan (e-mail: xianwu@med.nagoya-u.ac.jp).

with hypertension and dilated cardiomyopathy.[3,6–8] However, limited information has been available on cathepsin activation and its potential function in cardiac stiffening and ECM metabolism.

Both calcium channel blockers (CCBs) and angiotensin II type 1 receptor (AT_1R) blockers (ARBs) attenuate both cardiac dysfunction and ECM remodeling associated with HF in animal models.[2,9] Treatment of hypertensive patients with the combination of a CCB and an ARB has been shown to have a renoprotective effect and to be cost effective.[10] It has been reported that the combination of an ARB and a CCB has also shown to be a useful therapeutic strategy for the prevention of hypertensive heart failure.[11] However, the precise mechanisms underlying the cardioprotection afforded by the combination of a CCB and an ARB in animals or patients with hypertensive HF remain largely unknown. Oxidative stress is a hallmark of chronic HF, and the progression of cardiac hypertrophy to LV dysfunction can be prevented by treatment with antioxidants in animal models.[12,13] The cardiac and vascular protection conferred by CCBs and ARBs has been suggested to be attributable to antioxidant activity.

Dahl salt-sensitive (DS) rats are studied as a model of salt-sensitive hypertension in humans.[2,14] We have now investigated the changes in collagen and elastin expression and content and the relation between diastolic LV stiffness and the ratio of elastin to collagen in the LV of DS rats during the development of hypertensive HF. We have also examined the pharmacological mechanisms underlying the cardioprotection afforded by the combination of the ARB olmesartan (OLM) and the CCB azelnidipine (AZE) independently of the antihypertensive effect of these drugs in DS rats. We thus also treated DS rats fed a high-salt diet with the vasodilator hydralazine (HYD) or with apocynin (APO), an inhibitor of reduced nicotinamide adenine dinucleotide phosphate (NADPH) oxidase.

METHODS

Animals and Experimental Protocol

Male inbred DS rats were obtained from Japan SLC (Hamamatsu, Japan) and were handled in accordance with the guidelines of Nagoya University Graduate School of Medicine and with the Guide for the Care and Use of Laboratory Animals (National Institutes of Health publication no. 85-23, revised 1996). Weaning rats were fed laboratory chow containing 0.3% NaCl until 7 weeks of age. DS rats fed an 8% NaCl diet after 7 weeks manifest compensated concentric LV hypertrophy secondary to hypertension at 12 weeks and a distinct stage of fatal LV failure with lung congestion at 19 weeks.[3] DS rats were therefore fed an 8% NaCl diet from 7 weeks of age and were randomized to an untreated (HF) group, an HYD treatment group (10 mg/kg of body weight per day in drinking water), an OLM + AZE treatment group (3 and 6 mg/kg per day, respectively, in chow), and an APO treatment group (0.5 mmol/kg per day in drinking water) from 12 to 19 weeks of age (n = 10 for each group). APO was obtained from EMD Biosciences, Inc (La Jolla, CA), and both OLM and AZE were kindly provided by Sankyo Pharmaceutical, Co (Tokyo, Japan). DS rats fed a 0.3% NaCl diet after 7 weeks of age remain normotensive, and such animals served as age-matched controls (control group, n = 10). At 19 weeks of age, rats were anesthetized by intraperitoneal injection of ketamine (50 mg/kg) and xylazine (10 mg/kg) and were subjected to hemodynamic and echocardiographic analyses. The heart was subsequently excised, and LV tissue was either assayed for superoxide production, stored at −80°C for molecular analyses, or fixed with paraformaldehyde for pathological analysis.

Echocardiographic and Hemodynamic Analyses

Systolic blood pressure was measured weekly in conscious animals by tail-cuff plethysmography (BP-98A; Softron, Tokyo, Japan). At 19 weeks of age, rats were subjected to transthoracic echocardiography as previously described.[3] Echocardiography was performed with an SONOS 7500 ultrasound system and an ultraband transducer of 5–12 MHz (Philips, Andover, MA). LV end-diastolic (LVDd) and end-systolic (LVDs) dimensions and the thickness of the interventricular septum were measured. LV fractional shortening was calculated as 100% × (LVDd − LVDs)/LVDd. The peak negative myocardial velocity gradient (MVG) was derived from tissue Doppler imaging as a measurement of diastolic function. After echocardiography, a 2F micromanometer-tipped catheter (SPR-407; Millar Instruments, Houston, TX) that had been calibrated relative to atmospheric pressure was inserted through the right carotid artery into the LV. We evaluated the maximum first derivative of LV pressure (LV dP/dt_{max}) as an index of contractility, minimal rate of LV pressure change (LV dP/dt_{min}), and the pressure half-time ($T_{1/2}$) as an index of relaxation. Tracings of LV pressure and the electrocardiogram were digitized to determine the pressure half-time and LV end-diastolic pressure.

Quantitative Reverse Transcription–Polymerase Chain Reaction Analysis

Total RNA was isolated from LV tissue with the use of an RNeasy Fibrous Tissue Mini Kit (Qiagen, Inc, Valencia, CA) and was subjected to reverse transcription. The resulting complementary DNA was subjected to quantitative real-time polymerase chain reaction analysis with primers specific for monocyte chemoattractant protein (MCP)-1, connective tissue growth factor (CTGF), or osteopontin and with the use of an ABI 7300 Real-Time PCR System (Applied Biosystems, Foster City, CA), as previously described.[15,16] The amount of each messenger RNA (mRNA) was normalized by the corresponding amount of glyceraldehyde-3-phosphate dehydrogenase (GAPDH) mRNA.

Immunoblot Analysis

Tissue homogenates (50 μg of protein) were fractionated by sodium dodecyl sulfate–polyacrylamide gel electrophoresis, and the separated proteins were transferred to a polyvinylidene difluoride membrane (Amersham Pharmacia Biotech, Little Chalfont, Buckinghamshire, United Kingdom). The membrane was probed with antibodies to cathepsin S or cathepsin K[7,17]; to cathepsin L (Sigma-Aldrich, St. Louis,

MO); to MMP-12 (Epitomics, Inc., Burlingame, CA); or to type Iα collagen, type III collagen, or GAPDH (Santa Cruz Biotechnology, Santa Cruz, CA). Immune complexes were detected with the use of enhanced chemiluminescence reagents and were quantified by scanning densitometry (Bio-Rad, Hercules, CA). The amounts of target proteins were normalized by that of GAPDH.

Zymography

In vitro zymography was performed as previously described.[15] In situ zymography was performed with a kit (MMP In Situ Zymo-Film; Wako, Pure Chemical Industries, Ltd., Osaka Japan)[1] and in the absence or presence of the MMP inhibitor EDTA (1 μmol/L), the cathepsin inhibitor *trans*-epoxysuccinyl-L-leucylamido-(4-guanidino)butane (E64, 20 μmol/L), or the serine protease inhibitor phenylmethylsulfonyl fluoride (2 mmol/L).

Measurement of Collagen and Elastin

Elastin was quantified as previously described.[18] In brief, LV rings were defatted in acetone and dried, and proteins were extracted from the dried tissue by agitation in 0.3% sodium dodecyl sulfate for 12 hours. ECM proteins other than elastin (including collagen) were solubilized by three 15-minute extractions in 0.1 mol/L NaOH performed in a boiling water bath, and elastin was quantified on the basis of the dry weight of the residue. Collagen content was determined by measurement with the use of a colorimetric assay[19] of the amount of hydroxyproline in the NaOH supernatants after their evaporation and hydrolysis of the residue in 6 M HCl for 24 hours at 110°C.

Immunohistochemistry

LV tissue was fixed with ice-cold 4% paraformaldehyde for 16 to 24 hours, embedded in paraffin wax, and processed for immunohistochemistry as described.[3,16] In brief, transverse sections (3 μm) were cut with a cryostat and stained with a mouse monoclonal antibody that recognizes rat macrophages (1:100 dilution; Chemicon, Temecula, CA) or with rabbit polyclonal antibodies to mouse CTGF (Torrey Pines Biolabs, Houston, TX). As a negative control, primary antibodies were replaced with nonimmune immunoglobulin G.

Assay of Superoxide Production, Glutathione, and Angiotensin II

Superoxide (O_2^-) production by total homogenates of fresh LV tissue was measured with the use of a lucigenin-based enhanced chemiluminescence assay as described.[20] A low lucigenin concentration (5 μmol/L) was used to minimize artifactual O_2^- production attributable to redox cycling. In brief, homogenate protein (1 mg) in 1 mL of lysis buffer [20 mmol/L Tris–HCl (pH 7.5), 150 mmol/L NaCl, 1 mmol/L EDTA, 1 mmol/L ethylene glycol tetraacetic acid, and 1% Triton X-100] was transferred to an assay tube, and NADPH and dark-adapted lucigenin were added to final concentrations of 100 and 5 μmol/L, respectively, immediately before the measurement of chemiluminescence. All assays were performed in triplicate. The chemiluminescence signal was sampled every minute for 12 minutes with a tube luminometer (20/20; Turner Biosystems, Sunnyvale, CA), and the respective background counts were subtracted from the experimental values.

The amount of total glutathione [reduced (GSH) plus oxidized (GSSG)] in LV tissue was determined by the recycling assay based on glutathione reductase and 5,5'-dithiobis-(2-nitrobenzoic acid) as described.[21] Dihydroethidium staining for the production of superoxide was also performed as described.[22] In brief, myocardial sections (5 μm) cut with a cryostat were treated with acetone for 10 minutes and then incubated for 30 minutes at 37°C with 5 μmol/L dihydroethidium in phosphate-buffered saline. The sections were then examined with a laser scanning confocal microscope equipped with WinROOF version 5.0 image processing software (Mitani, Tokyo, Japan). The amount of angiotensin II in LV homogenates prepared in an ice-cold solution containing 25 mmol/L EDTA, 0.44 mmol/L 1,20-orthophenanthroline monohydrate, 1 mmol/L sodium parachloromercuribenzoate, and 3 μmol/L rat renin inhibitor acetyl-His-Pro-Phe-Val-Statine-Leu-Phe (WFML) was measured by radioimmunoassay and was normalized by LV weight.

Assay of Elastolytic Activity

Elastolytic activity in the myocardium was assayed as previously described.[3] Total LV homogenates (200 μg of protein) were incubated with fluorescein-conjugated DQ elastin (Molecular Probes, Eugene, OR) for 24 hours at 37°C, after which fluorescence was measured with a Fluoroskan Ascent CF instrument (Labsystems, Helsinki, Finland) at excitation and emission wavelengths of 485 and 530 nm, respectively. Data are presented as relative units after adjustment for background levels.

Statistical Analysis

Data were considered to be normally distributed and are presented as means ± SEM unless indicated otherwise. Differences were analyzed by Student *t* test or by 1-way analysis of variance followed by Scheffe multiple comparison test. A P value of <0.05 was considered statistically significant.

RESULTS

Hemodynamics and LV Structural and Functional Characteristics

At 19 weeks of age, neither heart rate nor body weight differed significantly among the 5 groups of DS rats (Table 1). Systolic blood pressure was higher in the HF group than in the control group at 8 weeks of age and thereafter (Fig. 1), whereas it was reduced in the HYD group and the OLM + AZE group at 13 weeks of age and thereafter compared with that in the HF group. There was no significant difference in systolic blood pressure between the HYD and OLM + AZE groups at 19 weeks of age ($P > 0.05$). The ratio of LV weight to body weight, an index of LV hypertrophy, was 59% greater in the HF group than in the control group at 19 weeks of age, and the increase in this parameter was attenuated by treatment with HYD, OLM + AZE, or APO (Table 1). Similarly, the ratio of lung wet weight to lung dry weight, an index of pulmonary congestion, was increased by 60% in HF rats compared with

TABLE 1. Hemodynamic, Echocardiographic, and Other Parameters for DS Rats in the 5 Experimental Groups at 19 Weeks of Age

Parameter	Control	HF	HYD	OLM + AZE	APO
Body weight (g)	417 ± 16	376 ± 24	406 ± 17	412 ± 19	401 ± 21
Heart rate (bpm)	416 ± 12	478 ± 23	501 ± 16	426 ± 18	450 ± 16
SBP (mm Hg)	151 ± 4	229 ± 3*	205 ± 208†	208 ± 5†	217 ± 6
LVW:BW (mg/g)	2.2 ± 0.1	3.5 ± 0.3*	2.7 ± 0.2†	2.4 ± 0.2‡	2.8 ± 0.3†
Lung weight (wet/dry)	4.2 ± 0.3	6.7 ± 0.5*	5.2 ± 0.4†	4.3 ± 0.3‡	4.9 ± 0.4†
IVST (mm)	1.4 ± 0.1	2.1 ± 0.1*	1.7 ± 0.1†	1.6 ± 0.1†	1.8 ± 0.1†
LVDd (mm)	7.1 ± 0.1	9.4 ± 0.4*	8.1 ± 0.2†	7.4 ± 0.2†	8.2 ± 0.3†
LVFS (%)	46 ± 1	34 ± 2*	43 ± 1†	48 ± 2†	41 ± 1†
dp/dt_{max} (mm Hg/s)	9284 ± 1124	7127 ± 927*	9467 ± 2034†	11,990 ± 1113‡	10,132 ± 2314†
dp/dt_{min} (mm Hg/s)	12,167 ± 1466	7796 ± 1019*	9039 ± 2405*	13,167 ± 917‡	10,800 ± 2014*†
$T_{1/2}$ (ms)	3.4 ± 0.1	5.5 ± 0.2*	4.9 ± 0.3*	3.7 ± 0.2‡	4.4 ± 0.2*†
LVEDP (mm Hg)	4.8 ± 0.5	16.5 ± 1.5*	14.5 ± 1.4*	6.9 ± 0.5‡	9.3 ± 1.5*†
Elastolytic activity	450 ± 56	1980 ± 134*	1810 ± 201*	750 ± 88†	1259 ± 109†
Ang II (pg/mg LVW)	155 ± 13	360 ± 43*	346 ± 51*	178 ± 45†	308 ± 65*

Elastolytic activity is expressed in fluorescence units. Data are means ± SEM for at least 6 animals of each group.
*$P < 0.05$ versus control group; †$P < 0.05$, ‡$P < 0.01$ versus HF group.
Ang II, angiotensin II; BW, body weight; IVST, interventricular septum; LVEDP, left ventricular end-diastolic pressure; LVFS, left ventricular fractional shortening; LVW, left ventricular weight; SBP, systolic blood pressure.

control rats, and this change was attenuated by treatment with HYD, OLM + AZE, or APO.

Both interventricular septum and LVDd were greater, whereas LV fractional shortening and LV dP/dt_{max} were smaller, in HF rats than in control rats. The changes in these parameters were inhibited by treatment with OLM + AZE and by that with HYD or APO (Table 1). The ratio of LV end-diastolic pressure and the $T_{1/2}$, an index of LV diastolic stiffness and relaxation, were also increased in the HF group, whereas the LV dP/dt_{min} was decreased in HF rats compared with control rats (Table 1). Treatment with OLM + AZE or with APO ameliorated all these changes in parameters of LV diastolic function, whereas HYD showed no benefit despite reducing systolic blood pressure by the same extent as did the combination therapy. Treatment with the combination of an ARB and a CCB thus inhibited LV remodeling, preserved LV systolic function, and attenuated LV diastolic dysfunction in a manner independent of its hypertensive action, and these effects were mimicked by treatment with APO.

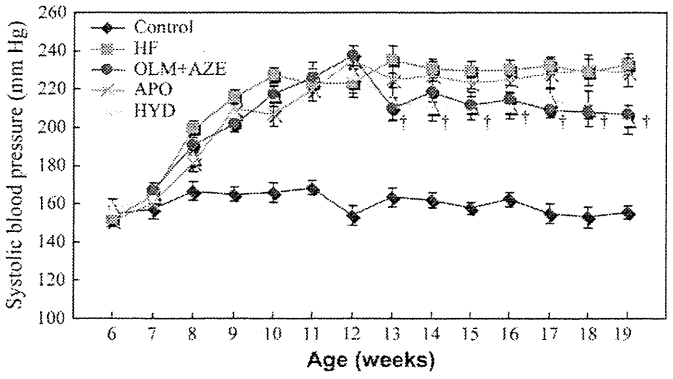

FIGURE 1. Time course of systolic blood pressure in DS rats fed a high-salt diet and either left untreated (HF) or treated with HYD, with the combination of OLM and AZE (OLM + AZE) or with apocynin (APO). Results are also shown for age-matched DS rats fed a low-salt diet (control). Data are means ± SEM for 10 rats of each group. †$P < 0.05$ for HYD or OLM + AZE groups versus HF group.

Myocardial Collagen and Elastin Expression and Content

Quantitative analysis of immunoblots revealed that the amounts of types Iα and III collagen in LV tissue were increased in the HF group compared with the control group and that these changes were inhibited by all 3 drug treatments (Figs. 2A, B). The type III:Iα collagen ratio, which is thought to be negatively correlated with cardiac stiffness, tended to be smaller in the HF group than in the control group, but this difference was not statistically significant (Fig. 2C). This ratio was significantly decreased in the HYD and APO groups, but not in the OLM + AZE group, compared with the control group. A colorimetric assay confirmed that the total amount of hydroxyproline derived from collagen hydrolysis was increased in the HF group and that this increase was attenuated by treatment with HYD, OLM + AZE, or APO (Fig. 2D). In contrast, the ratio of elastin to collagen content was decreased in the HF group compared with the control group, and this change was attenuated by treatment with OLM + AZE or with APO but not by that with HYD (Fig. 2E). The elastin to collagen ratio was positively correlated with the peak negative MVG (Fig. 2F), which is itself negatively correlated with diastolic cardiac stiffness.

Myocardial MMP and Cathepsin Expression and Activity

Immunoblot analysis revealed that the amounts of the active forms of cathepsin S (28 kDa), cathepsin K (29 kDa), and MMP-12 (45 kDa) in the LV were increased in HF rats compared with control rats and that these increases were

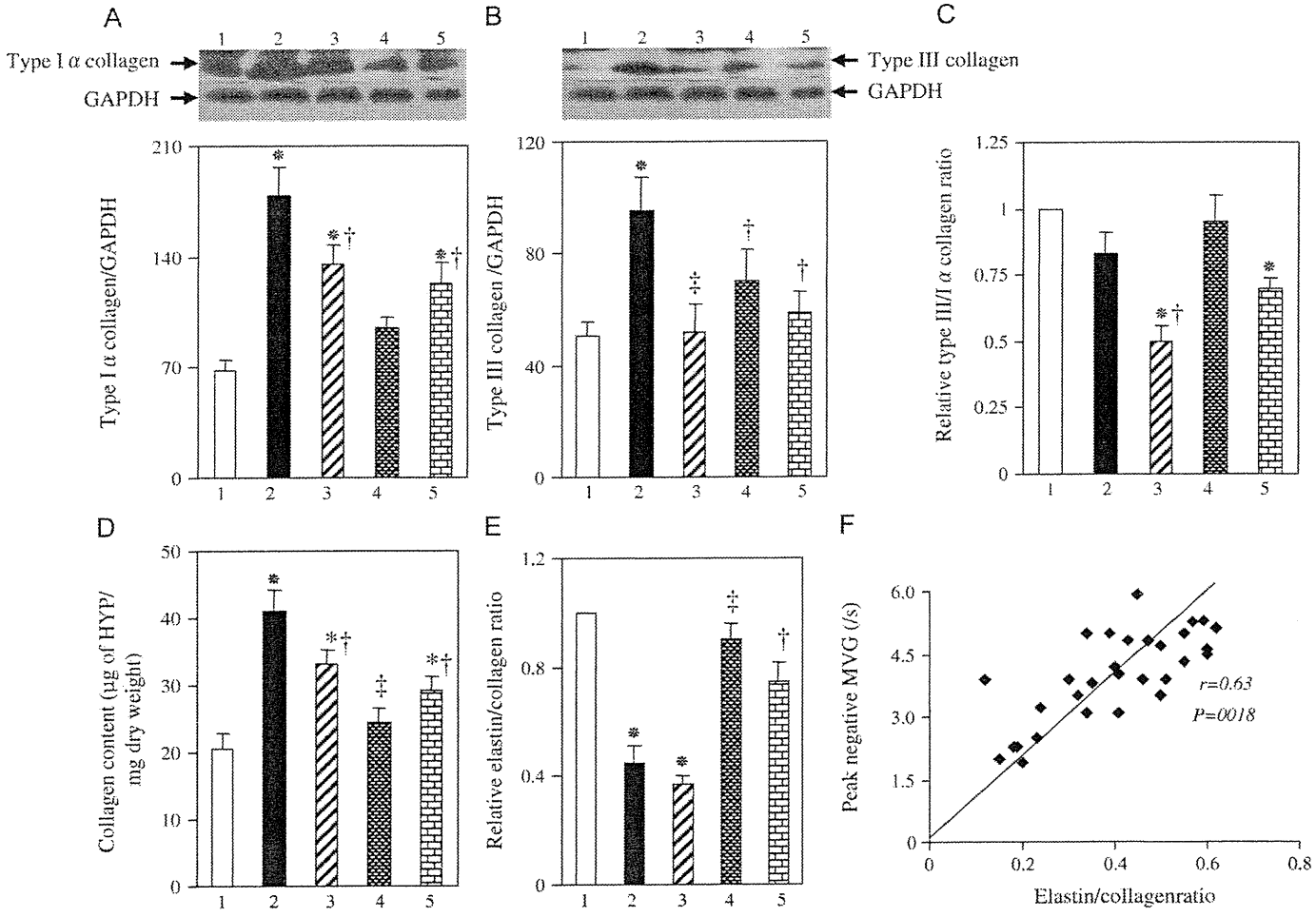

FIGURE 2. Collagen and elastin expression in the LV of DS rats in the 5 experimental groups at 19 weeks of age. A, B, Immunoblot analysis of type Iα (A) and type III (B) collagen in the LV of rats of the control (1), HF (2), HYD (3), OLM + AZE (4), or APO (5) groups. Representative blots and densitometric analysis of the collagen to GAPDH ratio are shown in the upper and lower panels, respectively. C, Type III:Iα collagen ratio determined from immunoblots similar to those shown in (A) and (B). Data are expressed relative to the value for the control group. D, E, Collagen content (D) and the ratio of elastin to collagen contents (E) of the LV. Data in (D) are expressed as micrograms of hydroxyproline (HYP) per milligram of tissue dry weight, whereas those in (E) are expressed relative to the value for the control group. F, Relation of peak negative MVG to the elastin to collagen ratio for 6 rats of each group. Quantitative data in (A) to (E) are means ± SEM for 6 rats per group. *$P < 0.05$ versus control group; †$P < 0.05$, ‡$P < 0.01$ versus HF group.

attenuated by treatment with OLM + AZE or APO (Figs. 3A–C). Consistent with these findings, elastolytic activity in the HF group was 4.4 times that in the control group, and this increase was attenuated in both OLM + AZE and APO groups (Table 1).

Gelatin zymography revealed major bands of 72 and 68 kDa for MMP-2 and 92 and 88 kDa for MMP-9 (Fig. 3D), corresponding to the latent and active forms, respectively, of these proteases,[15,23] in LV tissue. Quantitation of the data showed that the total gelatinolytic activity (pro plus active forms) of MMP-2 or MMP-9 was increased in the HF group relative to the control group and that these changes were suppressed by treatment with OLM + AZE or APO (Figs. 3E, F). The ratio of activated MMP-2 to total MMP-2, an index of net MMP-2 activation, was also increased in HF rats ($P < 0.05$) in a manner sensitive to treatment with OLM + AZE or APO (data not shown, $P < 0.05$). In situ zymography further confirmed that gelatinolytic activity was increased in HF rats (Fig. 3G); the activity was inhibited by EDTA and by E64 but not by phenylmethylsulfonyl fluoride, suggesting that it was attributable to MMPs and cysteine proteases rather than to serine proteases. HYD had no effect on the expression or activity of cathepsins or MMPs in the myocardium of DS rats fed a high-salt diet (Figs. 3A–F).

Myocardial Inflammation

Immunostaining revealed prominent macrophage infiltration in the LV of HF rats at 19 weeks of age (Figs. 4A, C). This infiltration was accompanied by increases in the abundance of mRNAs for MCP-1 and osteopontin (Figs. 4D, E). These inflammatory changes were attenuated by treatment with OLM + AZE or APO but not by that with HYD. The amounts of CTGF mRNA and protein were also increased in HF rats in a manner sensitive to treatment with OLM + AZE or APO but not to that with HYD (Figs. 4B, F).

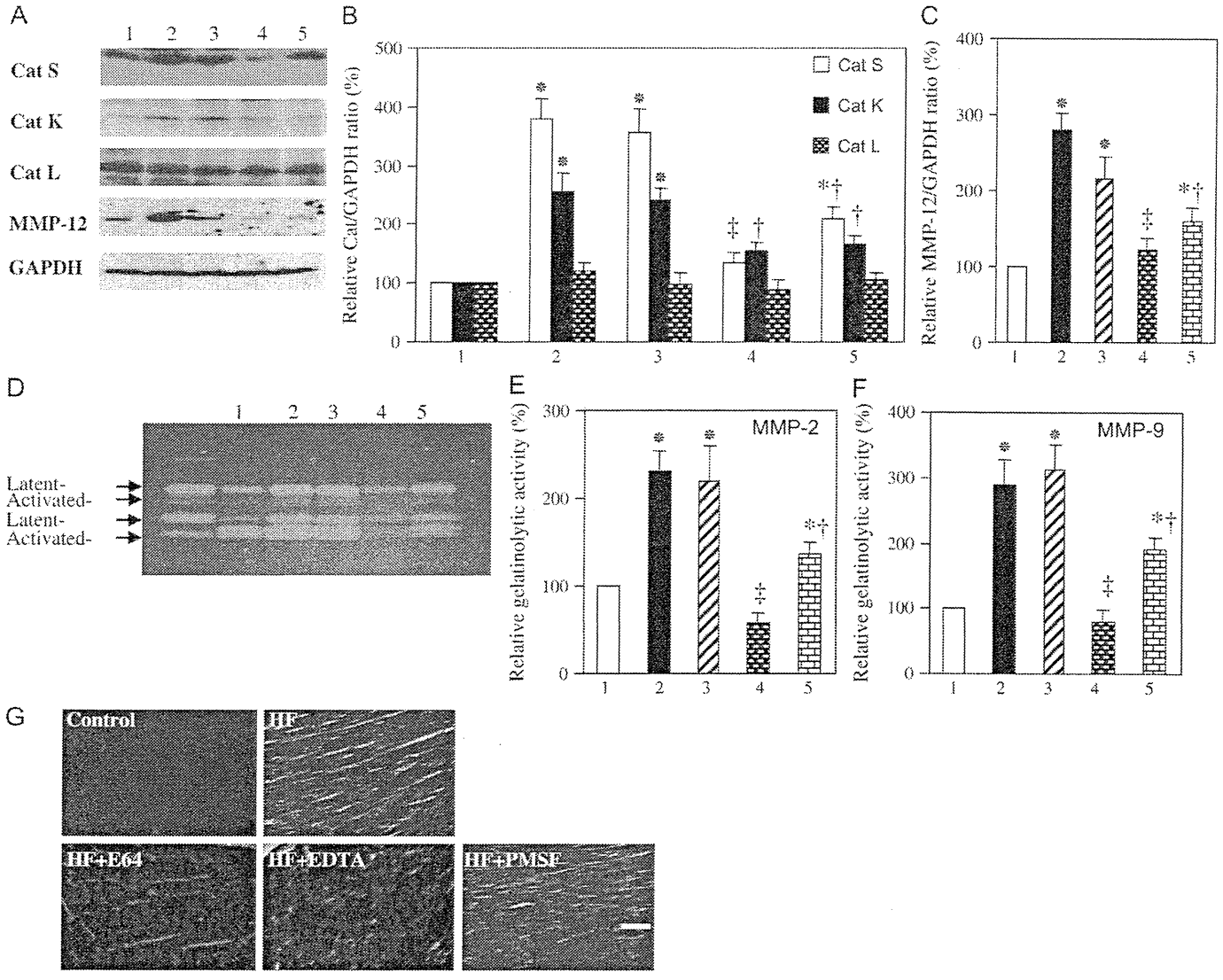

FIGURE 3. Expression and activity of MMPs and cathepsins in the LV of DS rats in the 5 experimental groups at 19 weeks of age. A, Immunoblot analysis of cathepsins (Cats) S, K, and L and MMP-12 in the LV of rats of the control (1), HF (2), HYD (3), OLM + AZE (4), or APO (5) groups. B, C, Densitometric analysis of each cathepsin/GAPDH (B) or MMP-12:GAPDH (C) ratio determined from immunoblots similar to those shown in (A). Data are expressed as a percentage of the corresponding value for the control group and are means ± SEM for 6 rats of each group. *$P < 0.05$ versus control group; †$P < 0.05$, ‡$P < 0.01$ versus HF group. D, Gelatin zymography of LV tissue homogenates. The 72- and 68-kDa bands for MMP-2 and the 92- and 88-kDa bands for MMP-9 correspond to the latent and active forms, respectively, of each protease. E, F, Total gelatinolytic activities of MMP-2 (E) and MMP-9 (F) were determined from quantitation of the latent and active forms of each protease in gels similar to that shown in (D). Data are expressed as a percentage of the corresponding value for the control group and are means ± SEM for 5 rats of each group. (G) In situ zymography of gelatinolytic activity in the LV of rats from the control and HF groups. Tissue from the HF rat was also incubated in the presence of EDTA (1 μmol/L), E64 (20 μmol/L), or PMSF (2 mmol/L). Brightness in the light microscopic images represents endogenous gelatinase activity. Scale bar: 50 μm. PMSF, phenylmethylsulfonyl fluoride.

Myocardial Oxidative Stress

Staining with dihydroethidium revealed that superoxide (O_2^-) production in myocardial tissue sections was increased in HF rats relative to that in control rats and that this increase was attenuated by treatment with OLM + AZE or APO but not by that with HYD (Fig. 5A). The NADPH oxidase–dependent production of O_2^- in LV tissue was also greater for HF rats than for control rats, and this increase was attenuated by treatment with OLM + AZE or APO but by that with HYD (Fig. 5B). The generation of O_2^- in LV homogenates of HF rats was largely abolished by the flavoprotein inhibitor diphenyleneiodonium (data not shown), suggesting that NADPH oxidase was indeed the likely source of the superoxide. The glutathione redox ratio (GSH:GSSG) was decreased in LV tissue of HF rats compared with control rats, and this change was prevented by treatment with OLM + AZE or APO but not

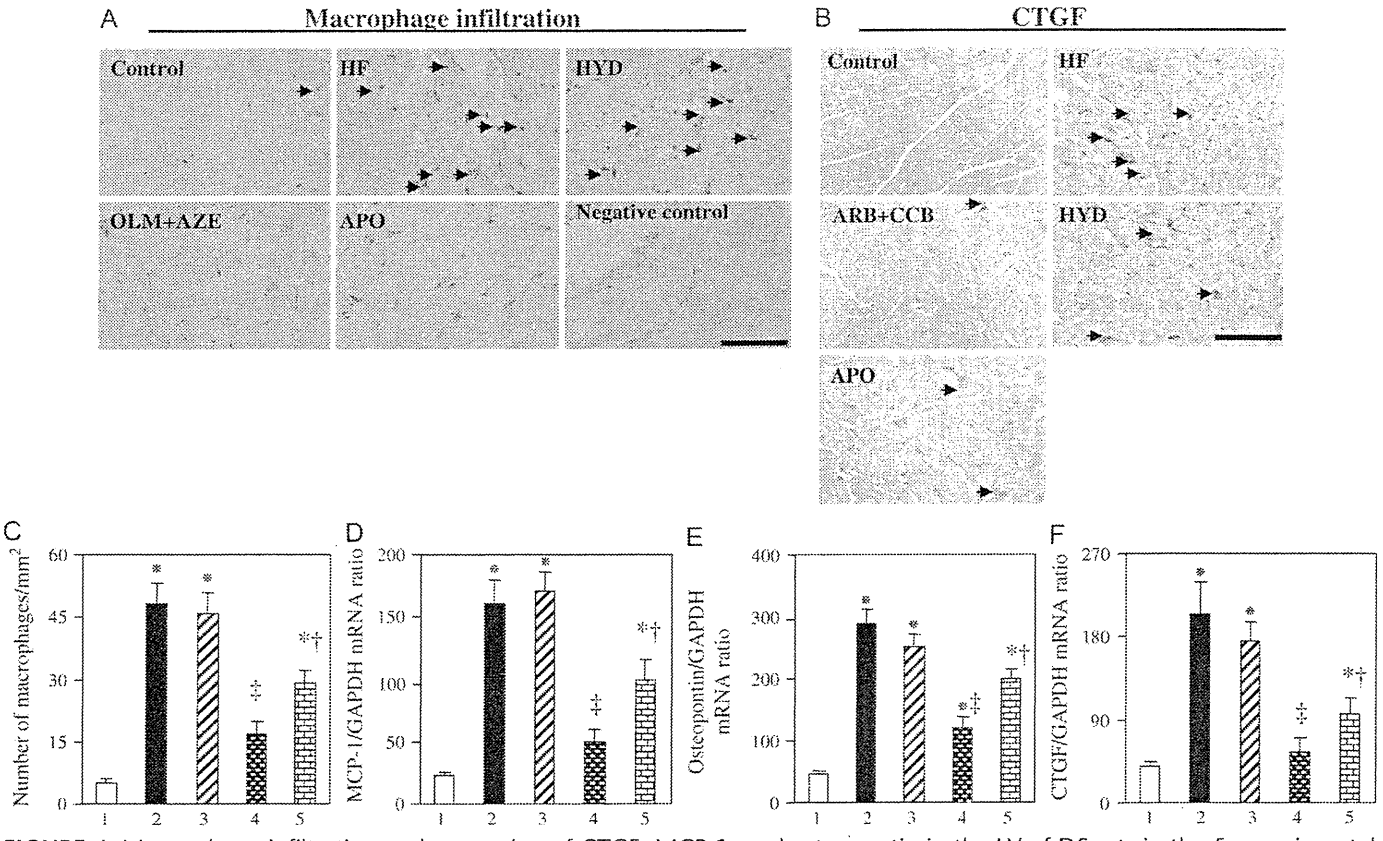

FIGURE 4. Macrophage infiltration and expression of CTGF, MCP-1, and osteopontin in the LV of DS rats in the 5 experimental groups at 19 weeks of age. A, C, Representative immunohistochemical staining for macrophage infiltration in the LV is shown in (A). A section from an HF rat stained with nonimmune immunoglobulin G instead of primary antibodies is shown as a negative control. Arrowheads indicate macrophages. Scale bar: 100 μm. Quantitation of the number of infiltrated macrophages per square millimeter is shown in (C). Data are means ± SEM for 6 rats of each group. *$P < 0.05$ versus control group; †$P < 0.05$, ‡$P < 0.01$ versus HF group. B, Representative immunohistochemical staining for CTGF in the LV. Arrowheads indicate immunoreactivity. Scale bar: 100 μm. D–F, Quantitative RT-PCR analysis of MCP-1, osteopontin, and CTGF mRNAs, respectively, in LV tissue of (1) control, (2) HF, (3) HYD, (4) OLM + AZE, and (5) APO groups. Data are means ± SEM for 6 rats of each group. RT-PCR, reverse transcription–polymerase chain reaction.

by that with HYD (Fig. 5C). Finally, the amount of angiotensin II in the LV was increased in HF rats relative to control rats in a manner sensitive to treatment with OLM + AZE but not to that with HYD or APO (Table 1).

DISCUSSION

We have made several important observations in the present study. First, failing myocardium of DS rats with hypertension is definitively characterized by an excessive diastolic LV stiffness associated with changes in the protein levels of collagen isoforms and decreases in the ratio of elastin protein to collagen protein. Second, NADPH oxidase is the responsible enzyme, and selective reduction of NADPH oxidase activity significantly reduced the activation and activity of elastolytic protease and local O_2^- generation in failing myocardium of DS rats. The APO-mediated antioxidative and anti-inflammatory effects are compatible with those in cardiac structural remodeling and diastolic dysfunction. Third, the administration of OLM + AZE to failing hearts in DS rats ameliorated LV remodeling and diastolic dysfunction concomitant with suppressed myocardial collagen accumulation, redressed the balance between elastin and collagen, decreased local O_2^- generation and inflammatory changes, and suppressed elastolytic protease activation and activity, whereas HYD showed no benefit despite similar decreases in blood pressure.

Collagen constitutes up to 85% of ECM in the heart, with the myocardial collagen network consisting predominantly of collagen types I and III.[24,25] Collagen type I confers rigidity, whereas collagen type III contributes to tissue elasticity. Collagen type I is thus thought to be a major determinant of myocardial stiffness,[24] and a decrease in the ratio of collagen type III to type I expression has been associated with increased myocardial stiffness.[4] However, previous studies have examined such changes in collagen isoform expression only at the mRNA level. We have now examined collagen expression by immunoblot analysis and determined collagen content by measurement of hydroxyproline derived from collagen hydrolysis. We found that the amounts of type Iα and type III collagen were significantly increased, whereas the type III to type Iα collagen ratio tended

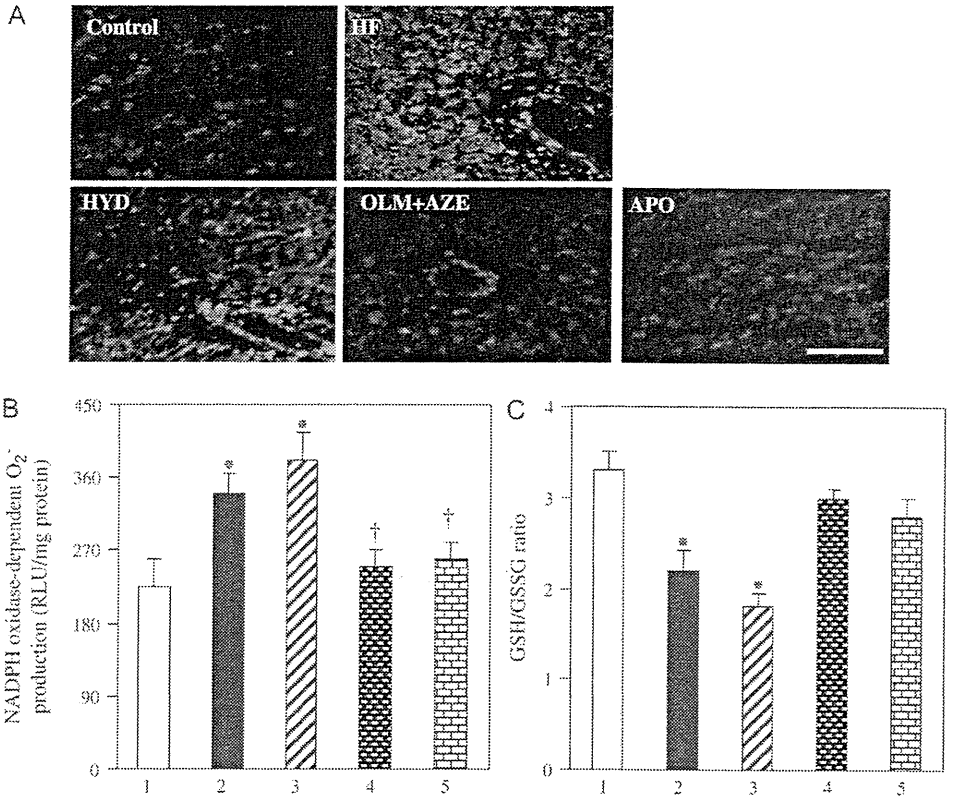

FIGURE 5. Oxidative stress in the LV of DS rats in the 5 experimental groups at 19 weeks of age. A, Representative dihydroethidium staining for superoxide production in LV sections. Scar bar: 100 μm. B, NADPH oxidase–dependent O_2^- production in LV homogenates prepared from rats of the (1) control, (2) HF, (3) HYD, (4) OLM + AZE, and (5) APO groups. Data are expressed as relative light units (RLU) per milligram of protein and are means ± SEM for 6 rats of each group. *$P <$ 0.05 versus control group; †$P <$ 0.05 versus HF group. C, The GSH:GSSG ratio in LV tissue. Data are means ± SEM for 6 rats of each group.

to be decreased, in HF rats. These findings demonstrated that the collagen type mRNA III to type I mRNA ratio may not be a good predictor of cardiac stiffness in this animal model of HF. A decrease in the elastin to collagen ratio has been proposed to be responsible for an increase in arterial stiffness in animals and humans.[18,26] We observed that the elastin to collagen ratio in the LV was decreased in HF rats and that this ratio was positively correlated with the peak negative MVG. Our findings demonstrated that the decrease in the elastin to collagen ratio underlies the increase in LV stiffness in DS rats with HF. The decrease in the elastin to collagen ratio associated with the development of HF was prevented by treatment with OLM + AZE or with APO but not by that with HYD.

Elastin degradation is thought to be mediated by MMPs and cathepsins.[6,27,28] Both MMP-2 and MMP-9 have previously been implicated in the development and progression of myocardial remodeling and in LV dilation.[1,5,29] We have now shown that treatment with OLM + AZE or APO inhibited the increases in cathepsin and MMP-12 expression, in the gelatinolytic activities of MMP-2 and MMP-9 and in total elastolytic activity associated with the development of HF in DS rats. MMP-9 and cathepsin S were previously shown to promote elastin disruption associated with atherosclerosis.[30,31] MMPs and cathepsins have also been shown to be produced by resident cardiac cells and to manifest marked collagenolytic and elastolytic activities.[6,7,17] Our findings demonstrated that treatment with OLM + AZE prevents LV fibrosis and the decrease in the elastin to collagen ratio through inhibition of the expression and activation of elastolytic proteases. The levels of CTGF mRNA and protein were also increased in the failing myocardium of DS rats, and these effects were ameliorated by treatment with OLM + AZE or APO. Upregulation of *CTGF* gene expression has previously been associated with HF,[16] and NADPH oxidase–dependent production of reactive oxygen species was shown to be responsible for an increase in *CTGF* gene expression in the aorta of diabetic mice.[32] *CTGF* gene expression is also rapidly increased on exposure of cardiac myocytes to prohypertrophic stimuli,[33] consistent with the notion that upregulation of this growth factor contributes to cardiac hypertrophy and fibrosis. The observed inhibition of *CTGF* gene expression by OLM + AZE in the myocardium of hypertensive DS rats, likely resulting from a reduction in the extent of NADPH oxidase–dependent superoxide production, may thus have contributed, at least in part, to the attenuation of cardiac ECM remodeling and HF.

A phagocyte-type NADPH oxidase is thought to serve as a prominent source of reactive oxygen species in the myocardium.[22] Superoxide generation by NADPH oxidase has also been shown to result in the activation of several proteases and to contribute to cardiac remodeling.[12,34] Our results now indicate that NADPH oxidase is a major source of O_2^- in the failing myocardium of DS rats and that selective inhibition of NADPH oxidase activity reduces not only the level of O_2^- but also the activity of elastolytic proteases (MMPs and cathepsins). These findings, together with previous observations suggesting that both CCBs and ARBs exert antioxidant activity[35,36] and that blockade of Ca^{2+} channels or angiotensin II action reduces the extent of proteolysis associated with various cardiovascular injuries,[30] suggest that the inhibition of

proteolysis resulting from the antioxidant activity of OLM + AZE is largely responsible for the cardioprotective effects of this drug combination. NADPH oxidase–derived O_2^- has been implicated as an important mediator of angiotensin II signaling.[37] Angiotensin II induces oxidative stress through the AT_1R-mediated activation of NADPH oxidase.[13] We found that the concentration of angiotensin II was increased in the myocardium of HF rats in a manner sensitive to treatment with OLM + AZE. The beneficial effects of OLM + AZE are thus likely also attributable to a reduction in AT_1R-mediated myocardial oxidative stress associated with a reduction in the local concentration of angiotensin II.

Oxidative stress induces the expression of redox-sensitive genes for chemoattractant proteins such as MCP-1 and for cell adhesion molecules. The superoxide anion is thought to function as a signaling molecule that mediates an increase in the activity of the transcription factor nuclear factor κB, which in turn contributes to the upregulation of such proinflammatory genes.[38] Macrophage infiltration into the failing myocardium of DS rats was accompanied by upregulation of the expression of *MCP-1* and osteopontin genes in the present study. The observation that these effects were abrogated by treatment with APO suggests that the myocardial inflammatory response is induced by activation of NADPH oxidase and contributes to the cardiovascular injury and fibrosis apparent in this model of HF. Macrophages play a key role in the production and release of MMPs and cathepsins associated with atherosclerosis.[39] Histochemical staining for macrophages in the failing myocardium of DS rats was previously shown to colocalize with that for MMP-2 and MMP-9, but the staining for MMP-2 and MMP-9 was not necessarily colocalized with that for macrophages.[1] We previously showed that the abundance of cathepsin S and cathepsin K mRNAs and proteins was markedly increased throughout the myocardium of DS rats with HF, with staining apparent in both cardiomyocytes and smooth muscle cells.[3] These findings demonstrated that macrophages contribute to the production and secretion of MMPs and cathepsins but are not the only cell type to express these proteases. Restraint of the inflammatory process by treatment with OLM + AZE thus likely contributes to the reduction in MMP and cathepsin expression induced by this drug combination.

Plasma renin, angiotensin II, and aldosterone levels were reportedly reduced in hypertensive DS rats.[16,40] It has recently been reported that local angiotensin-converting enzyme and AT_1R mRNA levels were upregulated in the LV of humans and rats with HF.[16,40] These observations suggested that the local angiotensin system in the LV myocardium may thus be activated in this low-renin hypertensive rat model. This notion is supported by our current observation that local tissue angiotensin II level in the LV myocardium was higher in DS HF rats than in control rats, and this change was reduced by treatment with OLM + AZE. Additionally, previous studies have shown that the primary dysfunction is in the kidney in DS rat model, and the development of LV failure parallels the deterioration of renal function.[41–44] Furthermore, it was demonstrated that impairment of renal dysfunction (specifically salt metabolism) plays an important role in the pathogenesis of HF.[44,45] These findings suggested that the beneficial effects of combination with OLM and AZE might be also attributable to improvement of salt/water balance or/and renal function in this model. Further investigations into these issues are required.

In summary, our findings suggest that changes in the expression of collagen isoforms and a decrease in the ratio of elastin to collagen may account for the increase in stiffness of the failing myocardium in DS rats. Furthermore, increased oxidative stress appears to be a driver for the activation of the elastolytic proteases. The observed cardioprotective effects of the combination of OLM (an ARB) and AZE (a CCB) are likely attributable, at least in part, to prevention of these changes in collagen isoform expression and the elastin to collagen ratio in the failing myocardium as a result of the inhibition of NADPH oxidase–dependent superoxide generation and inflammation.

REFERENCES

1. Sakata Y, Yamamoto K, Mano T, et al. Activation of matrix metalloproteinases precedes left ventricular remodeling in hypertensive heart failure rats: its inhibition as a primary effect of angiotensin-converting enzyme inhibitor. *Circulation*. 2004;109:2143–2149.
2. Kim S, Yoshiyama M, Izumi Y, et al. Effects of combination of ACE inhibitor and angiotensin receptor blocker on cardiac remodeling, cardiac function, and survival in rat heart failure. *Circulation*. 2001;103:148–154.
3. Cheng XW, Obata K, Kuzuya M, et al. Elastolytic cathepsin induction/activation system exists in myocardium and is upregulated in hypertensive heart failure. *Hypertension*. 2006;48:979–987.
4. Saka M, Obata K, Ichihara S, et al. Pitavastatin improves cardiac function and survival in association with suppression of the myocardial endothelin system in a rat model of hypertensive heart failure. *J Cardiovasc Pharmacol*. 2006;47:770–779.
5. Duhaney TA, Cui L, Rude MK, et al. Peroxisome proliferator-activated receptor alpha-independent actions of fenofibrate exacerbates left ventricular dilation and fibrosis in chronic pressure overload. *Hypertension*. 2007;49:1084–1094.
6. Cheng XW, Kuzuya M, Nakamura K, et al. Localization of cysteine protease, cathepsin S, to the surface of vascular smooth muscle cells by association with integrin αvβ3. *Am J Pathol*. 2006;168:685–694.
7. Shi GP, Sukhova GK, Kuzuya M, et al. Deficiency of the cysteine protease cathepsin S impairs microvessel growth. *Circ Res*. 2003;92:493–500.
8. Stypmann J, Glaser K, Roth W, et al. Dilated cardiomyopathy in mice deficient for the lysosomal cysteine peptidase cathepsin L. *Proc Natl Acad Sci U S A*. 2002;99:6234–6239.
9. Okuda N, Hayashi T, Mori, et al. Nifedipine enhances the cardioprotective effects of an angiotensin-II receptor blocker in an experimental animal model of heart failure. *Hypertens Res*. 2005;28:431–438.
10. Saito I, Kobayashi M, Matsushita Y, et al. Cost-utility analysis of antihypertensive combination therapy in Japan by a Monte Carlo simulation model. *Hypertens Res*. 2008;31:1373–1383.
11. Kim-Mitsuyama S, Izumi Y, Yoshhida K, et al. Additive beneficial of the combination of a calcium channel blocker and angiotensin blocker on a hypertensive rat-heart failure model. *Hypertens Res*. 2004;27:771–779.
12. Doerries C, Grote K, Hilfiker-Kleiner D, et al. Critical role of the NAD(P)H oxidase subunit p47phox for left ventricular remodeling/dysfunction and survival after myocardial infarction. *Circ Res*. 2007;100:894–903.
13. Gao L, Wang W, Li YL, et al. Sympathoexcitation by central ANG II: roles for AT1 receptor upregulation and NAD(P)H oxidase in RVLM. *Am J Physiol Heart Circ Physiol*. 2005;288:H2271–H2279.
14. Yoshida J, Yamamoto K, Mano T, et al. AT1 receptor blocker added to ACE inhibitor provides benefits at advanced stage of hypertensive diastolic heart failure. *Hypertension*. 2004;43:686–691.
15. Cheng XW, Kuzuya M, Nakamura K, et al. Mechanisms underlying the impairment of ischemia-induced neovascularization in matrix metalloproteinase 2-deficient mice. *Circ Res*. 2007;100:904–913.

16. Nagata K, Obata K, Xu J, et al. Mineralocorticoid receptor antagonism attenuates cardiac hypertrophy and failure in low-aldosterone hypertensive rats. *Hypertension*. 2006;47:656–664.
17. Cheng XW, Kuzuya M, Sasaki T, et al. Increased expression of elastolytic cysteine proteases, cathepsins S and K, in the neointima of balloon-injured rat carotid arteries. *Am J Pathol*. 2004;164:243–251.
18. Qiu H, Depre C, Ghosh K, et al. Mechanism of gender-specific differences in aortic stiffness with aging in nonhuman primates. *Circulation*. 2007; 116:669–676.
19. Behmoaras J, Osborne-Pellegrin M, Gauguier D, et al. Characteristics of the aortic elastic network and related phenotypes in seven inbred rat strains. *Am J Physiol Heart Circ Physiol*. 2005;288:H769–H777.
20. Maack C, Kartes T, Kilter H, et al. Oxygen free radical release in human failing myocardium is associated with increased activity of rac1-GTPase and represents a target for statin treatment. *Circulation*. 2003;108: 1567–1574.
21. Tietze F. Enzymic method for quantitative determination of nanogram amounts of total and oxidized glutathione: applications to mammalian blood and other tissues. *Anal Biochem*. 1969;27:502–522.
22. Tao L, Gao E, Jiao X, et al. Adiponectin cardioprotection after myocardial ischemia/reperfusion involves the reduction of oxidative/nitrative stress. *Circulation*. 2007;115:1408–1416.
23. Cheng XW, Kuzuya M, Nakamura K, et al. Mechanisms of the inhibitory effect of epigallocatechin-3-gallate on cultured human vascular smooth muscle cell invasion. *Arterioscler Thromb Vasc Biol*. 2005;25:1864–1870.
24. Heeneman S, Cleutjens JP, Faber BC, et al. The dynamic extracellular matrix: intervention strategies during heart failure and atherosclerosis. *J Pathol*. 2003;200:516–525.
25. Marijianowski MM, Teeling P, Mann J, et al. Dilated cardiomyopathy is associated with an increase in the type I/type III collagen ratio: a quantitative assessment. *J Am Coll Cardiol*. 1995;25:1263–1272.
26. Cattell MA, Anderson JC, Hasleton PS. Age-related changes in amounts and concentrations of collagen and elastin in normotensive human thoracic aorta. *Clin Chim Acta*. 1996;245:73–84.
27. Novinec M, Grass RN, Stark WJ, et al. Interaction between human cathepsins K, L, and S and elastins: mechanism of elastinolysis and inhibition by macromolecular inhibitors. *J Biol Chem*. 2007;282: 7893–7902.
28. Senior RM, Griffin GL, Fliszar CJ, et al. Human 92- and 72-kilodalton type IV collagenases are elastases. *J Biol Chem*. 1991;266:7870–7875.
29. Lebrasseur NK, Duhaney TA, De Silva DS, et al. Effects of fenofibrate on cardiac remodeling in aldosterone-induced hypertension. *Hypertension*. 2007;50:489–496.
30. Suganuma E, Babaev VR, Motojima M, et al. Angiotensin inhibition decreases progression of advanced atherosclerosis and stabilizes established atherosclerotic plaques. *J Am Soc Nephrol*. 2007;18:2311–2319.
31. Abdul-Hussien H, Soekhoe RG, Weber E, et al. Collagen degradation in the abdominal aneurysm: a conspiracy of matrix metalloproteinase and cysteine collagenases. *Am J Pathol*. 2007;170:809–817.
32. San Martin A, Du P, Dikalova A, et al. Reactive oxygen species-selective regulation of aortic inflammatory gene expression in type 2 diabetes. *Am J Physiol Heart Circ Physiol*. 2007;292:H2073–H2082.
33. Kemp TJ, Aggeli IK, Sugden PH, et al. Phenylephrine and endothelin-1 upregulate connective tissue growth factor in neonatal rat cardiac myocytes. *J Mol Cell Cardiol*. 2004;37:603–606.
34. Grote K, Flach I, Luchtefeld M, et al. Mechanical stretch enhances mRNA expression and proenzyme release of matrix metalloproteinase-2 (MMP-2) via NAD(P)H oxidase-derived reactive oxygen species. *Circ Res*. 2003;92:e80–e86.
35. Jinno T, Iwai M, Li Z, et al. Calcium channel blocker azelnidipine enhances vascular protective effects of AT1 receptor blocker olmesartan. *Hypertension*. 2004;43:263–269.
36. Tsuda M, Iwai M, Li JM, et al. Inhibitory effects of AT1 receptor blocker, olmesartan, and estrogen on atherosclerosis via anti-oxidative stress. *Hypertension*. 2005;45:545–551.
37. Zimmerman MC, Lazartigues E, Lang JA, et al. Superoxide mediates the actions of angiotensin II in the central nervous system. *Circ Res*. 2002;91: 1038–1045.
38. Collins T, Read MA, Neish AS, et al. Transcriptional regulation of endothelial cell adhesion molecules: NF-kappa B and cytokine-inducible enhancers. *FASEB J*. 1995;9:899–909.
39. Zalba G, Fortuno A, Orbe J, et al. Phagocytic NADPH oxidase-dependent superoxide production stimulates matrix metalloproteinase-9: implications for human atherosclerosis. *Arterioscler Thromb Vasc Biol*. 2007;27: 587–593.
40. Cheng XW, Murohara T, Kuzuya M, et al. Superoxide-dependent activation of cysteine protease cathepsin system is associated with hypertensive myocardial remodeling and represents a target for angiotensin II type 1 receptor blocker therapy. *Am J Pathol*. 2008;173:358–369.
41. Yamazaki K, Katoh H, Yamamoto N, et al. Characterization of new inbred strains of Dlah-Iwai salt-sensitive and salt-resistant rats. *Lab Anim Sci*. 1994;44:462–467.
42. Miura N, Suzuki S, Hamada Y, et al. Salt water promotes hypertension in Dahl-S rats. *Exp Anim*. 1999;48:289–292.
43. Tsunooka N, Morita H. Effect of a chronic high-salt diet on whole-body and organ sodium contents of Dahl rats. *J Hypertens*. 1997;15:851–856.
44. Klotz S, Hay I, Zhang G, et al. Development of heart failure in chronic hypertensive Dahl rats: focus on heart failure with preserved ejection fraction. *Hypertension*. 2006;47:901–911.
45. Maurer MS, King DL, El-Khoury Rumbarger L, et al. Left heart failure with a normal ejection fraction: identification of different pathophysiologic mechanisms. *J Card Fail*. 2005;11:177–187.

Atherosclerosis 206 (2009) 355–361

Contents lists available at ScienceDirect

Atherosclerosis

journal homepage: www.elsevier.com/locate/atherosclerosis

Statin prevents plaque disruption in apoE-knockout mouse model through pleiotropic effect on acute inflammation

Kae Nakamura[a], Takeshi Sasaki[a,b], Xian Wu Cheng[c,d], Akihisa Iguchi[a], Kohji Sato[b], Masafumi Kuzuya[a,*]

[a] Department of Geriatrics, Nagoya University Graduate School of Medicine, 65 Tsuruma-cho, Showa-ku, Nagoya 466-8550, Japan
[b] Department of Anatomy and Neuroscience, Hamamatsu University School of Medicine, 1 Handayama, Higashi-ku, Hamamatsu, Shizuoka, Japan
[c] Department of Cardiovascular Research Medicine, Nagoya University Graduate School of Medicine, Japan
[d] Department of Cardiology, Yanbian University Hospital, 119 Juzijie, Yanji, Jilin Province 133000, China

ARTICLE INFO

Article history:
Received 14 January 2009
Received in revised form 4 February 2009
Accepted 5 February 2009
Available online 21 February 2009

Keywords:
Atherosclerosis
Plaque
Inflammation
MMPs
Matrix protein

ABSTRACT

Although it has been demonstrated that statins stabilize atherosclerotic lesions in animal models of advanced atherosclerosis, there is little evidence to suggest that statins have a preventive effect on plaque rupture itself. In the present study, we examined the effect of fluvastatin on plaque disruption using a simple and quick method of plaque disruption in carotid artery lesions in apolipoprotein E-deficient mice. Male apolipoprotein E-deficient mice received normal chow and underwent ligation of the left common carotid artery just proximal to its bifurcation. Four weeks later, a polyethylene cuff was placed around the artery immediately proximal to the ligation site. Fluvastatin (10 mg/kg per day) was given by oral gavage every day starting at 3 days before cuff placement. The administration of fluvastatin suppressed atherosclerotic plaque disruption accompanied by luminal thrombi by 31.5% compared with controls at 4 days after the cuff was placed at the ligated carotid artery. Fluvastatin administration decreased matrix metalloproteinase-9 expression, gelatinolytic activity, endothelial adhesion molecules expression and neutrophil infiltration, and increased type I collagen content in the cuffed region. In summary, fluvastatin was found to prevent plaque disruption through pleiotropic effect on acute inflammation in an animal model using apolipoprotein E-deficient mice.

1. Introduction

Lipid lowering with statins, 3-hydroxy-3-methylglutaryl coenzyme A reductase inhibitors, has been established as an important therapy in the primary and secondary prevention of atherosclerotic disease [1,2]. However, in some clinical trials, statins have been found to reduce cardiovascular morbidity and mortality to a degree beyond what is expected from reductions in low-density lipoprotein cholesterol (LDL-C) levels alone [3,4], raising the possibility of clinically important effects beyond LDL-C reduction on cardiovascular disease [5]. In addition, recent studies have raised the additional possibility of positive short-term effects when statins are given to treat acute coronary syndrome (ACS) [6,7]. The significant benefits associated with the early initiation of statin treatment in ACS have added to the growing evidence supporting the hypothesis of pleiotropic effects of statins.

Plaque formation in the coronary arteries or plaque rupture in the peripheral vasculature in the later stages of atherosclerosis triggers the onset of acute ischemic events including myocardial and cerebral infarction. Although several plaque rupture models have been proposed, plaque rupture has been seen infrequently, even in old high serum cholesterol-prone mice after prolonged feeding with very high-cholesterol diets [8,9]. This means that intervention studies must necessarily involve weeks or even months of treatment, which is problematic in the case of agents that are scarce and/or expensive. Recently, we provided a novel, simple, fast and highly efficient model for the progress of atherosclerotic plaque vulnerability and disruption in apolipoprotein E-deficient (apoE-deficient) mice [10]. Although it has been demonstrated that statins stabilize atherosclerotic lesions in animal models of advanced atherosclerosis [11–13], there is little evidence to date that suggests that statins have a preventive effect on plaque disruption itself, with the exception of the report demonstrating plaque-stabilizing effects of pravastatin at brachiocephalic in apoE-deficient mice by Johnson et al. [14].

In the present study, we examined whether fluvastatin has a beneficial effect on plaque disruption by use of our novel mouse model.

* Corresponding author. Tel.: +81 52 744 2364; fax: +81 52 744 2371.
E-mail address: kuzuya@med.nagoya-u.ac.jp (M. Kuzuya).

0021-9150/$ – see front matter © 2009 Elsevier Ireland Ltd. All rights reserved.
doi:10.1016/j.atherosclerosis.2009.02.014

2. Materials and methods

2.1. Animals

All animal experiments were performed in accordance with the animal care guidelines of Nagoya University Graduate School of Medicine. Our experimental animals were 8-week-old apoE-deficient mice (C57BL/6) weighing between 21 and 25 g and purchased from Jackson Laboratory. The mice were provided with a standard diet (Oriental Yeast) and tap water ad libitum throughout the experimental period. Surgery was performed essentially as previously described [10]. In brief, the animals were anesthetized with an intraperitoneal (i.p.) injection of pentobarbital sodium (50 mg/kg; Dainippon Pharmaceutical). Ligation of the left common carotid artery in 9-week-old mice was performed just proximal to the bifurcation, following the procedure described previously. Four weeks after ligation, a polyethylene cuff was applied just proximal to the ligated site.

2.2. Experimental design and tissue collection

The mice were randomly assigned to one of two groups: the control group (vehicle; 0.5% carboxymethylcellulose) and the fluvastatin group (10 mg/kg per day). Dose of fluvastatin was referred to the previous report [15]. The treatments were given by oral gavage every day starting at 3 days before cuff placement. At various time points, mice were anesthetized by i.p. pentobarbital injection and blood samples were collected in heparinized syringes. The carotid arteries in the cuff were harvested for analysis by several methods and were processed as described below. Fluvastatin was supplied by Novartis Pharma AG.

2.3. Histological and immunohistochemical staining

Just before cuff placement (day 0) and 2 or 4 days after cuff placement, mice were perfused through the left cardiac ventricle with isotonic saline and 4% paraformaldehyde in 0.01 M phosphate buffer (pH 7.4) under physiological pressure. Carotid arteries were collected and processed for histological analysis as described previously [16]. Cross-cryosections (6 μm) were prepared from the intracuff region of each carotid artery and stained routinely with hematoxylin and eosin (H&E), and picrosirius red for collagen. The corresponding sections on separate slides were used for immunohistochemical staining. The sections were preincubated with 5% serum and then incubated with antibodies against neutrophils (1:50; Serotec) and matrix metalloproteinase (MMP)-9 (1:100; BIOMOL International LP). Immunohistochemical staining was visualized using an ABC Kit (Vector Laboratories) following the manufacturer's instructions. Levamisole (Vector Laboratories) was used as the inhibitor of endogenous alkaline phosphatase. Counterstaining for the nucleus was performed with Mayer's hematoxylin.

2.4. Morphometric analysis

All morphometric analyses were made on H&E stained sections. Histological classification of the plaque disruption at the intracuff region of the carotid artery was done according to previously published methods [11]. Briefly, the lesions were divided into three groups, based on the analyses of 30 sections at 60-μm intervals in each sample tissue. When there were no cracks and no mural or occlusive thrombus at the intracuff region, we classified them into "no disruption". When intraplaque hemorrhage, or mural or occlusive thrombus with cracks or erosion in the plaques were detected, these were classified into "hemorrhage" or "disruption", respectively.

2.5. Determination of collagen and neutrophils content

Collagen content was evaluated by the picrosirius red-stained positive area which appears bright when viewed with polarized light. Neutrophils infiltrated in the intima were assessed by the neutrophils positive area which was stained by anti-neutrophil antibody (1:50; Serotec, MCA771GA). For the quantification of collagen content and infiltration of neutrophils in the sections, National Institutes of Health Image software was used for all images. We set a threshold to automatically compute the positive areas for each stain and then computed the ratio of positive area to the intimal area.

2.6. Double immunofluorescence

Colocalization studies were performed with double immunofluorescence staining methods. The sections were preincubated with 5% serum and incubated with antibodies against MMP-9 (1:100; BIOMOL), neutrophils, and/or macrophages (1:100; BD Pharmingen) for 18 h. Immunoreactivity was visualized using a fluorescein-conjugated anti-rabbit IgG (1:100; Vector Laboratories) or Texas Red-conjugated anti-rat IgG (1:100; Vector Laboratories). The slides were mounted in glycerol-based Vectashield medium (Vector Laboratories) containing the nucleus stain 4′,6-diamidino-2-phenylindole (DAPI).

2.7. Real-time reverse transcription-polymerase chain reaction

Just before and 1, 2 or 4 days after cuff placement, carotid arteries from the intracuff region were collected without perfusing with 4% paraformaldehyde and soaked in RNA*later* (Ambion). Total RNA was extracted using a Qiagen RNeasy Micro Kit (Qiagen, Inc.) following the manufacturer's instructions. Quantitative real-time reverse transcription-polymerase chain reaction (RT-PCR) analysis using the Taqman method and the ABI 7300 real-time PCR System (Applied Biosystems) was performed as described previously [17]. The sequences of the primers and probes are shown in Table 1; glyceraldehyde 3-phosphate dehydrogenase (GAPDH) was measured in parallel with genes of interest and used as an internal standard.

2.8. In situ zymography

Gelatinolytic activity was analyzed using an MMP *in situ* Zymo-Film (Wako, Inc.). An MMP-PT *in situ* Zymo film containing 1,10-phenanthroline as an MMP inhibitor to block protease activity was used as a control. Just before and 4 days after cuff placement, tissues were collected from the intracuff region without perfusing with 4% paraformaldehyde, and were then frozen immediately in optimum cutting temperature (OCT) compound (Sakura Finetechnical). Frozen sections (4 μm) were placed on the film and incubated for 30 h at 37 °C in a moisture box following the manufacturer's instructions. The specimens were then stained with Amido black 10B (Sigma) for 15 min and destained for 10 min. The areas of gelatinolytic activity were visualized under a light microscope.

2.9. Statistical analysis

Data were represented as means ± S.E.M. One- or two-way analysis of variance (ANOVA) followed by post hoc testing (Scheffe test) or chi-squared test was used for statistical analysis where appropriate at $P < 0.05$.

Table 1
Taqman primer and probe sequences used in real-time PCR analysis.

Gene	Forward primer sequence	Reverse primer sequence	Probe sequence
Matrix metalloproteinase-2 (MMP-2)	CCCCATGAAGCCTTGTTTACC	TTGTAGGAGGTGCCCTGGAA	CAATGCTGATGGACAGCCCTGCA
Matrix metalloproteinase-3 (MMP-3)	CATGGAGACTTTGTCCCTTTTGAT	CGTCAAAGTGAGCATCTCCATTA	TGGCTCATGCCTATGCACCTGGAC
Matrix metalloproteinase-9 (MMP-9)	AGACCAAGGGTACAGCCTGTTC	GGCACGCTGGAATGATCTAAG	CGCACGAGTTCGGCCATGCAC
Matrix metalloproteinase-14 (MMP-14)	GTCAGCCTGCTTCTCATGTCC	CCACGCCACTGCGCTT	CGGATGTAGGCATAGGGCACTTCTCG
Tissue inhibitor of metalloproteinases 1 (TIMP-1)	GCCTACACCCCAGTCATGGA	GGCCCGTGATGAGAAACTCTT	TGGATATGCCCACAAGTCCCAGAACC
Tissue inhibitor of metalloproteinases 2 (TIMP-2)	GTCCCATGATCCCTTGCTACA	TGCCCATTGATGCTCTTCTCT	CTCCCCGGATGAGTGCCTCTGGA
Collagen type I	AGGCGAAGGCAACAGTCG	GTTCCGGYGTGACTCGTGC	ACCTACAGCACCCTTGTGGACGGC
Intercellular adhesion molecule 1 (ICAM-1)	CCCCGCAGGTCCAATTC	CCAGAGCGGCAGAGCAA	CACTGAATGCCAGCTCGGAGGATCAC
Vascular cell adhesion molecule 1 (VCAM-1)	ACAAAACGATCGCTCAAATCG	GGTGACTCGCAGCCCGTA	CTCCATGGCCCTCACTTGCAGCA
P-selectin	GCAAAGGCATAACATCACTTCCTG	AAAGCTTCCCAGGTGGTGTTG	AGTCCGATGCCCTGCCCTCACGA
E-selectin	TGTACGTCCTCTGGAGAGTGG	GCAGGGTGGGTCAAAGCTTC	CGCCTGCTCCAGCCTGCCATGTG

3. Results

3.1. The effect of statin on plaque disruption in carotid arteries

There were no differences in plasma total cholesterol levels between the fluvastatin and control groups (21.7 ± 1.5 mmol/L, $n = 33$ vs. 18.8 ± 1.1 mmol/L, $n = 32$; $P = 0.1$).

Before cuff placement (day 0), no significant differences in the histological findings at the equivalent sites of the cuffed region of the carotid artery were observed between the fluvastatin and control groups (Fig. 1A and B). At 4 days after cuff placement, the proportions of intraplaque hemorrhage and disruption in the neointima accompanying the intramural thrombus were compared between the fluvastatin and control groups. Fluvastatin administration was found to suppress atherosclerotic plaque disruption by 31.5% compared with controls at 4 days after cuff placement at the ligated carotid artery (Table 2, Fig. 1C and D), although no difference in the rate of intraplaque hemorrhage was detected between these two groups (Table 2).

Table 2
Fluvastatin reduces in percentage of plaque disruption in the murine model.

	n	Disruption	No disruption	
			Hemorrhage	No hemorrhage
Fluvastatin	25	24.0 (6)	36.0 (9)	40.0 (10)
Control	18	55.5 (10)	38.9 (7)	5.6 (1)

Tissue sections were classified into three groups based on our analysis of 30 sections at 60-μm intervals in each sample tissue. Disruption, presence of mural or occlusive thrombus with cracks or erosion in the plaques; hemorrhage, presence of intraplaque hemorrhage; no disruption and no hemorrhage, no cracks and no mural or occlusive thrombus. Data: %(n). $P < 0.05$ (chi-squared test).

3.2. Messenger RNA quantification

The levels of MMP-2, -3, -9 and -14, tissue inhibitor of metalloproteinases (TIMP)-1 and -2, type I collagen, vascular cell adhesion molecule (VCAM)-1, intercellular adhesion molecule (ICAM)-1, E-selectin, and P-selectin mRNAs were determined by quantitative real-time RT-PCR (Fig. 2). An increase in MMP-9 mRNA was

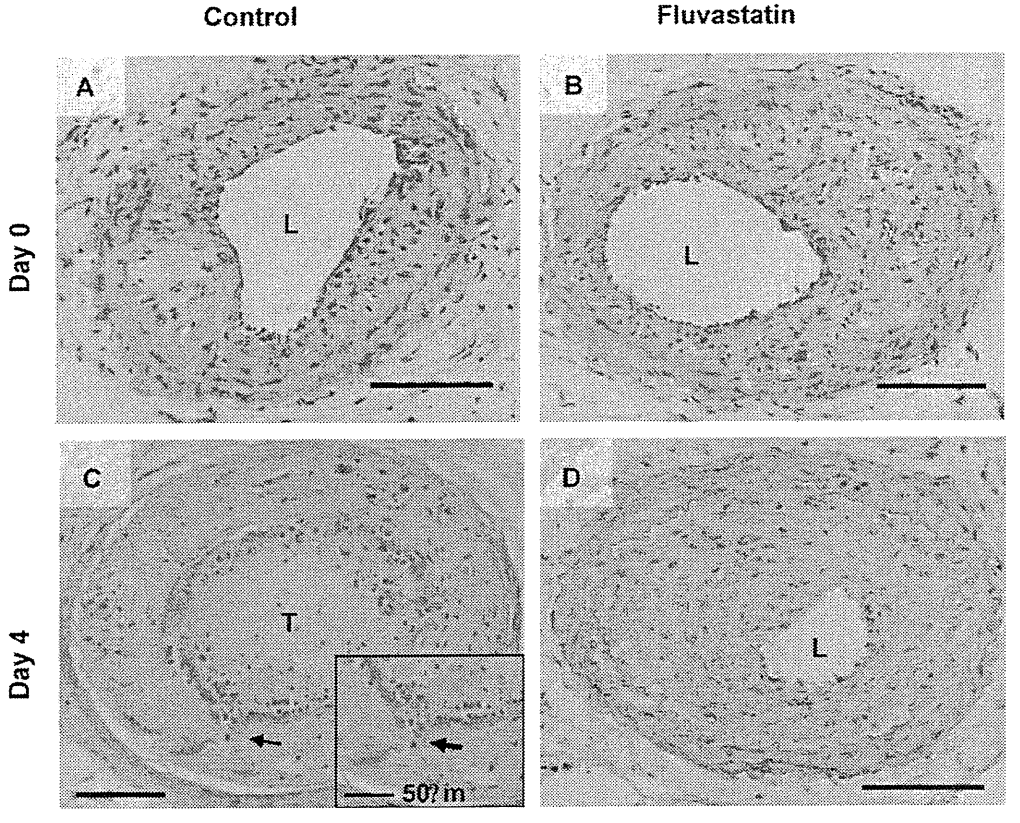

Fig. 1. The effect of fluvastatin on plaque disruption formation in the left carotid arteries of apoE-deficient mice. A through D, H&E staining of cross-sections of the left carotid artery. A and C, control; B and D, fluvastatin treatment; day 0, just before cuff placement; day 4, at days 4 after cuff placement. Bars = 100 μm. T (C) indicates thrombus, L (A and B) indicates lumen and arrow (C and inset) indicates the crack of fibrous cap.

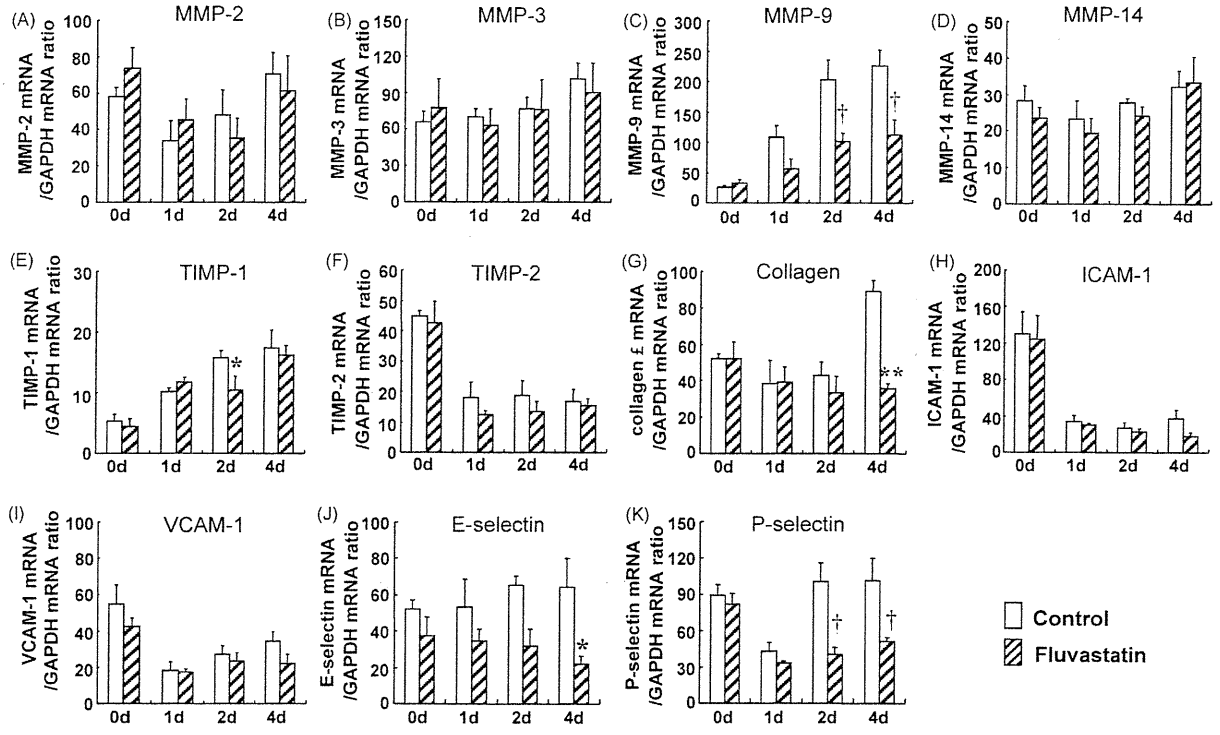

Fig. 2. Quantitative real-time RT-PCR analysis of the mRNAs for MMP-2 (A), MMP-3 (B), MMP-9 (C), MMP-14 (D), TIMP-1 (E), TIMP-2 (F), type I collagen (G), ICAM-1 (H), VCAM-1 (I), E-selectin (J), and P-selectin (K) in the left carotid arteries of fluvastatin-treated ($n = 5$) or control mice ($n = 5$) at the indicated time points. All data were normalized according to GAPDH mRNA; means ± S.E.M.; $^{*}P < 0.05$, $^{**}P < 0.01$, $^{\dagger}P < 0.001$.

observed at days 1, 2 and 4 after cuff placement in control mice, and this increase was significantly suppressed by fluvastatin at days 2 and 4 after cuff placement (Fig. 2C). The mRNA expression of MMP-2, -3 and -14 did not differ between the fluvastatin and control groups in the cuffed artery during the follow-up period after cuff placement (Fig. 2A, B and D). No significant differences were observed in TIMP-1 or -2 mRNA levels up to 4 days after cuff placement, with the exception of TIMP-1 mRNA levels at day 2. The amount of type I collagen mRNA was significantly suppressed at 4 days after cuff placement in the fluvastatin group compared with controls (Fig. 2E and G), although there was no significant difference in TIMP-2 mRNA between these groups (Fig. 2F). E-selectin and P-selectin mRNA levels were significantly suppressed by fluvastatin (Fig. 2J and K), although no statistical differences were detected in VCAM-1 and ICAM-1 mRNA levels between the fluvastatin and control groups (Fig. 2H and I).

3.3. *In situ zymography*

In situ zymographic analysis revealed gelatinolytic activity primarily in the neointimal region in control carotid arteries at 4 days after cuff placement (Fig. 3A), and this activity was suppressed in the carotid arteries of fluvastatin-treated mice (Fig. 3B). No gelatinolytic activity was observed in control specimens containing phenanthroline (Fig. 3C and D).

3.4. *Collagen content in the neointima*

There was no difference in collagen content between the fluvastatin and control groups just before cuff treatment (Fig. 3E, F and I). Although a significant decrease in collagen content was observed in control carotid arteries at day 4 compared with levels before cuff placement (Fig. 3G), the administration of fluvastatin successfully maintained the collagen content in the carotid artery after cuff placement (Fig. 3H).

3.5. *Neutrophil infiltration in the neointima*

Neutrophil infiltration was increased at days 2 and 4 after cuff placement at the ligated artery in the control group (Fig. 4A–C and E). The administration of fluvastatin was found to have significantly suppressed the neutrophil-positive area in the neointima of the carotid artery compared with controls at 4 days after cuff placement (Fig. 4D).

3.6. *MMP-9 localization*

Immunohistochemical analysis revealed that more intense MMP-9 staining was observed at the plaque region and in the atheromatous lesions in control carotid arteries at 2 days after cuff placement compared with the fluvastatin-treated group (Fig. 5A–E and H). Double labeling of sections of carotid arteries with antibodies to the macrophage- or neutrophil-specific markers (Fig. 5F and I, respectively) and MMP-9 revealed that MMP-9 was colocalized with macrophages and neutrophils (Fig. 5G and J, respectively).

4. Discussion

A number of studies have demonstrated that statins reduce MMP protein expression and activities when administered to hyperlipidemic animals, and that this is accompanied by changes in plaque morphology consistent with increased stability [11–13]. Moreover, the plaque-stabilizing effects of statins in animal models can apparently be obtained even independently of cholesterol lowering [12,13], which implies a direct effect of statins on the mechanisms leading to plaque instability. However, there is little direct evidence of the beneficial effects of statin on plaque rupture. Recently, Johnson et al. reported the interesting finding that pravastatin treatment prevents early plaque rupture in the brachiocephalic arteries of apoE-knockout mice, which demonstrated a direct beneficial effect on plaque stability [14].

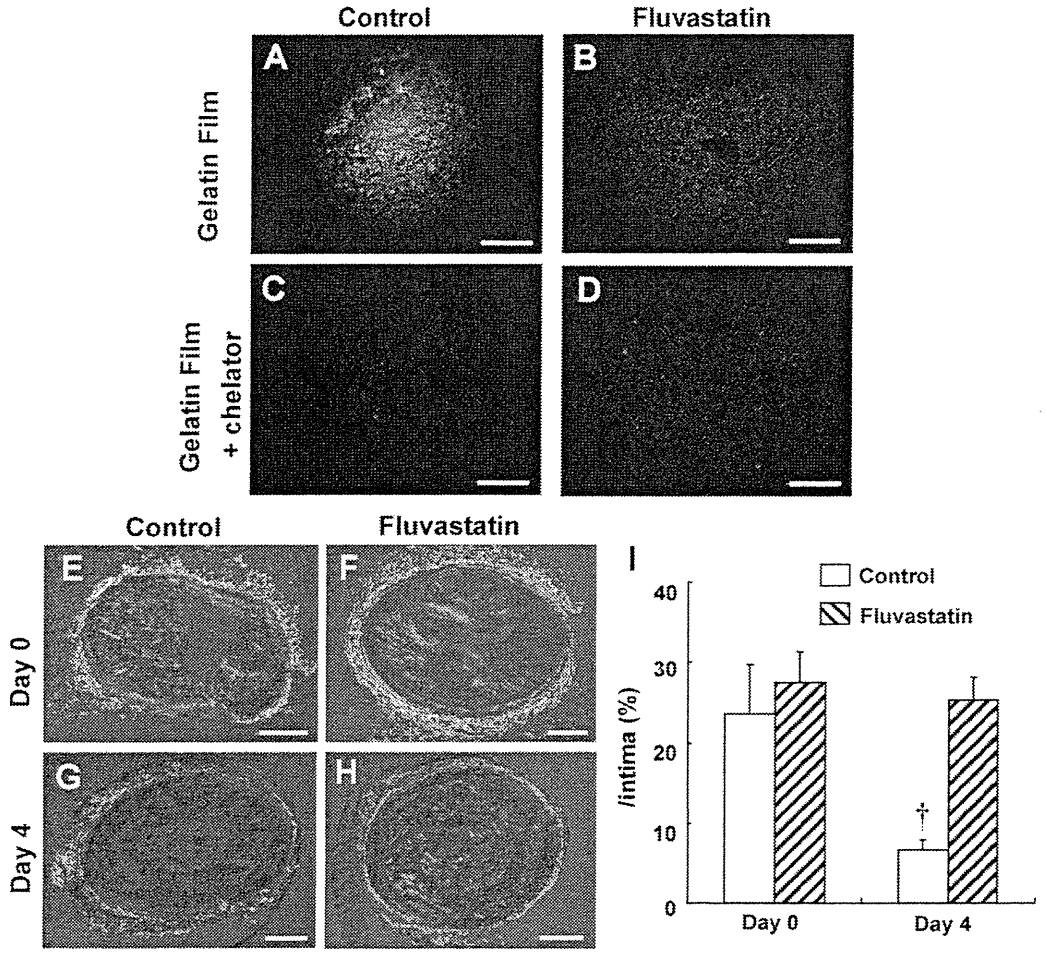

Fig. 3. Gelatinolytic activity and collagen content in the left carotid arteries in the fluvastatin and control groups. A through D, *in situ* zymography at 4 days after cuff placement. Brightness under a light microscope shows degradation with gelatinases. A and B: gelatin film; C and D: gelatin film with a chelator serving as a negative control. Bars = 100 μm. E through H, picrosirius red staining of specimens viewed under polarized light before cuff placement (day 0) and at 4 days after cuff placement. I, quantitative analysis of collagen content. Data were determined by computer analysis and were expressed as a percentage of the positive area for picrosirius red staining within the intima. Values are means ± S.E.M.; $n = 5$ (fluvastatin, day 0), $n = 16$ (fluvastatin, day 4), $n = 5$ (control, day 0), $n = 14$ (control, day 4), $^{\dagger}P < 0.001$. (For interpretation of the references to color in this figure legend, the reader is referred to the web version of the article.)

In the present study, we observed that fluvastatin reduced the rate of plaque disruption with mural thrombosis in our mouse model. As previously demonstrated [12–14], statin use has no effect on lipid levels in apo-E-deficient mice, suggesting that this effect of fluvastatin on plaque disruption in the present model is independent of plasma cholesterol lowering. It should be noted that fluvastatin administration had no effect on the induction of intraplaque hemorrhage after cuff placement, suggesting that this type of hemorrhage may not stem from plaque disruption but from intraplaque microvessels. In fact, recent studies in human and animal model have suggested that intraplaque hemorrhage was observed in atherosclerotic plaque regions, which is thought to be

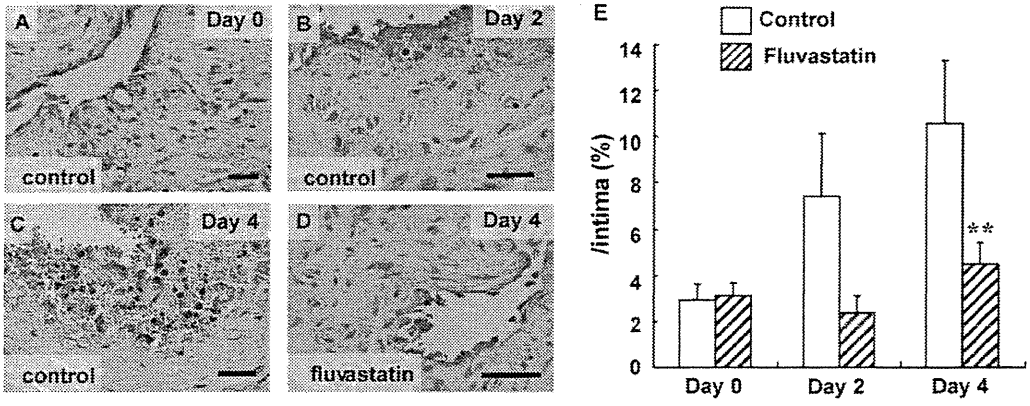

Fig. 4. Infiltration of neutrophils in the left carotid arteries before and after cuff placement. Immunoreactivity of neutrophils at day 0 (A), day 2 (B) and day 4 (C) in the control group after cuff placement, and at day 4 after cuff placement in the fluvastatin group (D). E, percentage of the neutrophil-positive area within the total intimal area. Values are means ± S.E.M. Fluvastatin group, $n = 12$ (day 0), $n = 10$ (day 2), $n = 14$ (day 4); control group, $n = 10$ (day 0), $n = 6$ (day 2), $n = 14$ (day 4), $^{**}P < 0.01$.

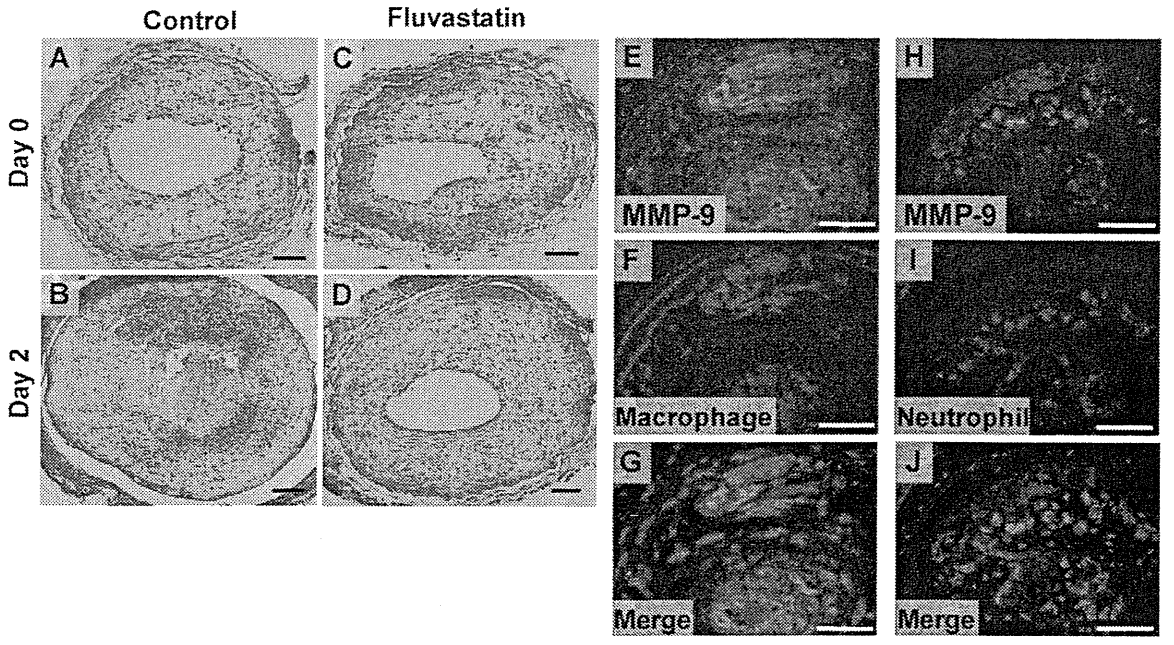

Fig. 5. Immunostaining of MMP-9 and identification of MMP-9-positive cells using immunofluorescent staining in the neointimal lesions of carotid arteries at days 0 and 2 after cuff placement. Immunoreactivity of MMP-9 at day 0 in the control (A) and fluvastatin (C) groups and at day 2 in the control (B) and fluvastatin (D) groups. Double fluorescence staining for MMP-9 was detected in the neointima and colocalized with markers of macrophages (F and G) and neutrophils (I and J) at day 2 in the control. Bars = 50 μm.

caused by rupture of the fragile and tortuous neovessels formed within the plaque [18–22].

The reduction of the plaque disruption rate by fluvastatin administration was associated with the preservation of collagen content as well as with a reduction in gelatinolytic activities in the vascular wall, which were decreased and enhanced, respectively, after cuff placement. It is assumed that proteinases, such as the MMP or cathepsin family, in the plaque are responsible for the plaque vulnerability, thereby favoring plaque rupture [23–27].

However, the exact proteinase involved in the destabilization of plaque remains uncertain. In the present study, we observed that fluvastatin decreased MMP-9 mRNA expression in the plaque between days 2 and 4 after cuff placement. In addition, the results of the time course of mRNA expression of major MMPs suggest that MMP-9 might play an important role in the process of plaque vulnerability, at least in this model. In fact, MMP-9 was deposited in the plaque lesions, and colocalized with macrophages and neutrophils. However, it is possible that other proteinases are also involved in plaque vulnerability. It should be noted that we observed a decrease in type I collagen mRNA expression in fluvastatin-treated disrupted regions compared with those in control mice; this is consistent with previous *in vitro* observations, which have demonstrated that statin, including fluvastatin, suppresses type I collagen mRNA in various cell types [28,29]. Nevertheless, much high contents of collagen were detected in the fluvastatin group, suggesting that proteolytic activity in the disruption-prone region was strongly attenuated by fluvastatin treatment.

TIMPs are a family of naturally occurring specific inhibitors of MMPs whose activity in atherosclerotic plaques seems to correlate with decreased MMP activity and hence reduced matrix remodeling [30,31]. In the present study, we observed that fluvastatin had no effect on TIMP-1 or -2 mRNA expression with the exception of TIMP-1 mRNA expression at day 2, which is consistent with the previous observation by Luan et al. that lovastatin has no effect on TIMP-1 or -2 secretion or on mRNA expression in rabbit smooth muscle cells (SMCs) [32]. The present results further confirm that fluvastatin reduced gelatinase activity in the intima through the reduction of MMP-9 expression.

The present results clearly show that neutrophil infiltration into the vascular wall after cuff placement was significantly attenuated by fluvastatin treatment. We also observed that fluvastatin suppressed ICAM-1 and VCAM-1 mRNA expression after cuff placement, although this difference did not reach statistical significance. In addition, fluvastatin significantly reduced the E-selectin and P-selectin mRNA levels in cuffed arteries. These results are consistent with those of previous reports demonstrating that statins inhibit interactions between leukocytes and endothelial cells through a reduction in adhesion molecule expression [33–36], and also decrease the number of inflammatory cells within atherosclerotic plaques and ischemic tissues [37,38].

Some phenotypic characteristics of plaques, such as collagen content, necrotic core size, the SMCs/macrophage ratio and fibrous cap thickness, have been widely used as indirect indicators of their stability [39]. Long-term administration of statins leads to this phenotype [11–13], resulting in plaque stability. In the study by Johnson et al., long-term treatment with pravastatin inhibits acute plaque rupture, which occurs at high frequency in the brachiocephalic arteries of male apoE-deficient mice after 8–40 weeks of fat feeding [14]. They showed that long-term treatment with pravastatin causes an increase in fibrous cap thickness and a decrease in plaque lipid content, suggesting that long-term statin treatment leads to changes in plaque phenotypes in apoE-deficient mice. However, in the present model, we found that the relatively short-term administration of statin may act directly on cells, contributing to the process of cuff-induced plaque disruption rather than statin-induced phenotypic changes in arterial walls. In fact, no phenotypic changes in plaques were observed after fluvastatin administration for 3 days just before cuff placement. The observed beneficial effects of short-term statin use are similar to the acute benefits associated with the early initiation of statin treatment in ACS [6,7].

In the present study, although we used the dose of fluvastatin for mice that was comparable with plasma fluvastatin concentration accomplished after oral administration of its clinical doses (10–20 mg) in humans [15], the implication of the present study may be restricted to this dose. Thus, further studies will be necessary to study several doses, which would confirm the physiological

and clinical relevance of this model. It must be noted that the present model does not completely reproduce human plaque rupture, the final event in a long and complex pathophysiological process. However, this model appears to be analogous to the events that occur to some extent in human plaque rupture: a reduction in collagen content, the presence of MMPs, and an increase in apoptotic cells and inflammatory cells in the plaque lesions before thrombosis formation, followed by neointima cracks and thrombotic occlusion of the artery at the site of the presumed rupture [10]. In the present study, these processes leading to plaque disruption seem to be inflammatory responses triggered by the cuff placement. Statin appears to prevent plaque disruption through the reduction of inflammatory responses, including leukocyte infiltration and MMP-9 expression, which are also observed in human plaque rupture regions. However, it is possible that other observed pleiotropic effects of statins, such as improved endothelial function [40] and reduced thrombogenic response [41,42], may be involved in the statin effect.Acknowledgments

This work was supported by a research grant from the Scientific Research Fund of the Ministry of Education, Science, and Cultures, Japan (No. 17590723). Nakamura K is a research fellow of the Japanese Society for the Promotion of Science (No. 19.8913).

References

[1] Shepherd J, Cobbe SM, Ford I, et al. Prevention of coronary heart disease with pravastatin in men with hypercholesterolemia. N Engl J Med 1995;333:1301–7.
[2] Scandinavian Simvastatin Survival Study Group. Randomised trial of cholesterol lowering in 4444 patients with coronary heart disease: the Scandinavian Simvastatin Survival Study (4S). Lancet. 1994;344:1383–9.
[3] Sacks FM, Moyeï LA, Davis BR, et al. Relationship between plasma LDL concentrations during treatment with pravastatin and recurrent coronary events in the Cholesterol and Recurrent Events trial. Circulation 1998;97:1446–52.
[4] Simes RJ, Marschner IC, Hunt D, et al. LIPID Study Investigators, relationship between lipid levels and clinical outcomes in the Long-term Intervention with Pravastatin in Ischemic Disease (LIPID) Trial. To what extent is the reduction in coronary events with pravastatin explained by on-study lipid levels? Circulation 2002;105:1162–9.
[5] Lefer AM, Scalia R, Lefer DJ. Vascular effects of HMG CoA-reductase inhibitors (statins) unrelated to cholesterol lowering: new concepts for cardiovascular disease. Cardiovasc Res 2001;49:281–7.
[6] Schwartz GG, Olsson AG, Ezekowitz MD, et al. Effects of atorvastatin on early recurrent ischemic events in acute coronary syndromes: the MIRACL study. A randomized controlled trial. JAMA 2001;285:1711–8.
[7] Cannon CP, Braunwald E, McCabe CH, et al. Intensive versus moderate lipid lowering with statins after acute coronary syndromes. N Engl J Med 2004;350:1495–504.
[8] Rosenfeld ME, Polinsky P, Virmani R, et al. Advanced atherosclerotic lesions in the innominate artery of the apoE knockout mouse. Arterioscler Thromb Vasc Biol 2000;20:2587–92.
[9] Calara F, Silvestre M, Casanada F, et al. Spontaneous plaque rupture and secondary thrombosis in apolipoprotein E-deficient and LDL receptor-deficient mice. J Pathol 2001;195:257–63.
[10] Sasaki T, Kuzuya M, Nakamura K, et al. A simple method of plaque rupture induction in apolipoprotein E-deficient mice. Arterioscler Thromb Vasc Biol 2006;26:1304–9.
[11] Fukumoto Y, Libby P, Rabkin E, et al. Statins alter smooth muscle cell accumulation and collagen content in established atheroma of watanabe heritable hyperlipidemic rabbits. Circulation 2001;103:993–9.
[12] Bea F, Blessing E, Bennett B, et al. Simvastatin promotes atherosclerotic plaque stability in ApoE-deficient mice independently of lipid lowering. Arterioscler Thromb Vasc Biol 2002;22:1832–7.
[13] Williams JK, Sukhova GK, Herrington DM, et al. Pravastatin has cholesterol-lowering independent effects on the artery wall of atherosclerotic monkeys. J Am Coll Cardiol 1998;31:684–91.
[14] Johnson J, Carson K, Williams H, et al. Plaque rupture after short periods of fat feeding in the apolipoprotein E-knockout mouse: model characterization and effects of pravastatin treatment. Circulation 2005;111:1422–30.
[15] Hayashidani S, Tsutsui H, Shiomi T, et al. Fluvastatin, a 3-hydroxy-3-methylglutaryl coenzyme A reductase inhibitor. Attenuates left ventricular remodeling and failure after experimental myocardial infarction. Circulation 2002;105:868–73.
[16] Sasaki T, Kuzuya M, Cheng XW, et al. A novel model of occlusive thrombus formation in mice. Lab Invest 2004;84:1526–32.
[17] Kuzuya M, Nakamura K, Sasaki T, et al. Effect of MMP-2 deficiency on atherosclerotic lesion formation in apoE-deficient mice. Arterioscler Thromb Vasc Biol 2006;26:1120–5.
[18] Jeziorska M, Woolley DE. Local neovascularization and cellular composition within vulnerable regions of atherosclerotic plaques of human carotid arteries. J Pathol 1999;188:189–96.
[19] Virmani R, Kolodgie FD, Burke AP, et al. Atherosclerotic plaque progression and vulnerability to rupture: angiogenesis as a source of intraplaque hemorrhage. Arterioscler Thromb Vasc Biol 2005;25:2054–61.
[20] Langheinrich AC, Michniewicz A, Sedding DG, et al. Correlation of vasa vasorum neovascularization and plaque progression in aortas of apolipoprotein E−/−/low-density lipoprotein−/− double knockout mice. Arterioscler Thromb Vasc Biol 2006;26:347–52.
[21] Shiomi M, Fan J. Unstable coronary plaques and cardiac events in myocardial infarction-prone Watanabe heritable hyperlipidemic rabbits: questions and quandaries. Curr Opin Lipidol 2008;19:631–6.
[22] Wilson SH, Herrmann J, Lerman LO, et al. Simvastatin preserves the structure of coronary adventitial vasa vasorum in experimental hypercholesterolemia independent of lipid lowering. Circulation 2002;105:415–8.
[23] Brown DL, Hibbs MS, Kearney M, et al. Identification of 92-kD gelatinase in human coronary atherosclerotic lesions: association of active enzyme synthesis with unstable angina. Circulation 1995;91:2125–31.
[24] Molloy KJ, Thompson MM, Jones JL, et al. Unstable carotid plaques exhibit raised matrix metalloproteinase-8 activity. Circulation 2004;110:337–43.
[25] Newby AC. Dual role of matrix metalloproteinases (matrixins) in intimal thickening and atherosclerotic plaque rupture. Physiol Rev 2005;85:1–31.
[26] Rodgers KJ, Watkins DJ, Miller AL, et al. Destabilizing role of cathepsin S in murine atherosclerotic plaques. Arterioscler Thromb Vasc Biol 2006;26:851–6.
[27] Lutgens E, Lutgens SP, Faber BC, et al. Disruption of the cathepsin K gene reduces atherosclerosis progression and induces plaque fibrosis but accelerates macrophage foam cell formation. Circulation 2006;113:98–107.
[28] Siegel-Axel DI, Runge H, Seipel L, et al. Effects of cerivastatin on human arterial smooth muscle cell growth and extracellular matrix expression at varying glucose and low-density lipoprotein levels. J Cardiovasc Pharmacol 2003;41:422–33.
[29] Riessen R, Axel DI, Fenchel M, et al. Effect of HMG-CoA reductase inhibitors on extracellular matrix expression in human vascular smooth muscle cells. Basic Res Cardiol 1999;94:322–32.
[30] Fabunmi RP, Sukhova GK, Sugiyama S, et al. Expression of TIMP-3 in human atheroma and regulation in lesion-associated cells: a potential protective mechanism in plaque stability. Circ Res 1998;83:270–8.
[31] Zaltsman AB, George SJ, Newby AC. Increased secretion of tissue inhibitors of metalloproteinases-1 and -2 from the aortas of cholesterol fed rabbits partially counterbalances increased metalloproteinase activity. Arterioscler Thromb Vasc Biol 1999;19:1700–7.
[32] Luan Z, Chase AJ, Newby AC. Statins inhibit secretion of metalloproteinases-1, -2, -3, and -9 from vascular smooth muscle cells and macrophages. Arterioscler Thromb Vasc Biol 2003;23:769–75.
[33] Pruefer D, Scalia R, Lefer AM. Simvastatin inhibits leukocyte–endothelial cell interactions and protects against inflammatory processes in normocholesterolemic rats. Arterioscler Thromb Vasc Biol 1999;19:2894–900.
[34] Sadeghi MM, Collinge M, Pardi R, et al. Simvastatin modulates cytokine-mediated endothelial cell adhesion molecule induction: involvement of an inhibitory G protein. J Immunol 2000;165:2712–8.
[35] Pruefer D, Makowski J, Schnell M, et al. Simvastatin inhibits inflammatory properties of *Staphylococcus aureus* alpha-toxin. Circulation 2002;106:2104–10.
[36] Nubel T, Dippold W, Kleinert H, et al. Statins inhibit high glucose-mediated neutrophil-endothelial cell adhesion through decreasing surface expression of endothelial adhesion molecules by stimulating production of endothelial nitric oxide. Microvasc Res 2003;65:118–24.
[37] Tiefenbacher CP, Kapitza J, Dietz V, et al. Reduction of myocardial infarct size by fluvastatin. Am J Physiol Heart Circ Physiol 2003;285:H59–64.
[38] Yamakuchi M, Greer JJ, Cameron SJ, et al. HMG-CoA reductase inhibitors inhibit endothelial exocytosis and decrease myocardial infarct size. Circ Res 2005;96:1185–92.
[39] Rekhter MD. How to evaluate plaque vulnerability in animal models of atherosclerosis? Cardiovasc Res 2002;54:36–41.
[40] O'Driscoll G, Green D, Taylor RR. Simvastatin, an HMG-coenzyme A reductase inhibitor, improves endothelial function within 1 month. Circulation 1997;95:1126–31.
[41] Eto M, Kozai T, Cosentino F, et al. Statin prevents tissue factor expression in human endothelial cells: role of Rho/Rho-kinase and Akt pathways. Circulation 2002;105:1756–9.
[42] Bickel C, Rupprecht HJ, Blankenberg S, et al. Influence of HMGCoA reductase inhibitors on markers of coagulation, systemic inflammation and soluble cell adhesion. Int J Cardiol 2002;82:25–31.

European Journal of Pharmacology 615 (2009) 163–170

Contents lists available at ScienceDirect

European Journal of Pharmacology

journal homepage: www.elsevier.com/locate/ejphar

Cardiovascular Pharmacology

Long-term administration of nifedipine attenuates cardiac remodeling and diastolic heart failure in hypertensive rats

Takashi Yamada [a], Kohzo Nagata [b,*], Xian Wu Cheng [a], Koji Obata [c], Masako Saka [c], Masaaki Miyachi [b], Keiko Naruse [c], Takao Nishizawa [a], Akiko Noda [b], Hideo Izawa [a], Masafumi Kuzuya [a,d], Kenji Okumura [a], Toyoaki Murohara [a], Mitsuhiro Yokota [c]

[a] Department of Cardiology, Nagoya University Graduate School of Medicine, Nagoya, Japan
[b] Department of Medical Technology, Nagoya University School of Health Sciences, 1-1-20 Daikominami, Higashi-ku, Nagoya 461-8673, Japan
[c] Department of Genome Science, Aichi-Gakuin University School of Dentistry, Nagoya, Japan
[d] The Department of Geriatrics, Nagoya University Graduate School of Medicine, Nagoya Japan

ARTICLE INFO

Article history:
Received 21 October 2008
Received in revised form 25 April 2009
Accepted 26 May 2009
Available online 6 June 2009

Keywords:
Hypertension
Fibrosis
Diastolic heart failure
Oxidative stress
Calcium channel blocker

ABSTRACT

The Ca^{2+} channel blocker nifedipine has been reported to reduce the rate of new overt heart failure. We investigated the effects of nifedipine on left ventricular remodeling, oxidative stress, and gene expression in the failing heart of Dahl salt-sensitive (DS) rats. DS rats fed a high-salt diet from 7 weeks of age were treated with a non-antihypertensive (1 mg/kg per day, Nif-L) or mild-antihypertensive dose of nifedipine (3 mg/kg per day, Nif-H) or with vehicle (Vehicle) from 12 to 19 weeks. Marked left ventricular hypertrophy and fibrosis were apparent and the ratio of collagen type I to type III mRNA levels and the activity of matrix metalloproteinase (MMP)-2 and its mRNA expression in the myocardium were increased in Vehicle at 19 weeks in comparison with Control. Load-induced left ventricular hypertrophy was reduced in Nif-H, but not in Nif-L, relative to that in Vehicle. Treatment with either dose of nifedipine reduced the extent of fibrosis, the collagen type I to type III mRNA ratio, and MMP-2 activity and its mRNA expression compared with those in Vehicle. The decrease in the ratio of reduced to oxidized glutathione and the increase in NADPH oxidase activity apparent in the left ventricle of Vehicle were also inhibited by nifedipine at both doses. Nifedipine thus inhibited the development of left ventricular fibrosis and diastolic heart failure in DS rats, independently of its antihypertensive effect. The overall protective action of nifedipine is likely attributable to its antioxidant effect as well as to its antihypertensive action.

1. Introduction

Hypertension is a major risk factor for cardiovascular disease and leads to coronary endothelial dysfunction and myocardial perfusion abnormalities. In addition, the cardiac hypertrophy and fibrosis that develop as an adaptive response to pressure overload are predictive of progressive heart disease and morbidity (Devereux and Roman, 1999), having been associated with ischemic heart disease, arrhythmia, and sudden death (Katz, 1990). Progressive changes in myocardial structure and function, referred to as myocardial remodeling, occur in response to chronic hemodynamic overload. Such remodeling is characterized by ventricular hypertrophy and enlargement, changes in chamber geometry, and pump dysfunction. Early changes in cardiac function may include left ventricular diastolic dysfunction, which has a poor prognosis and is often manifested in individuals with hypertension. About 30 to 40% of cases of heart failure occur in patients with preserved systolic function (Senni et al., 1998; Vasan et al., 1999), with diastolic dysfunction implicated as a major contributor to heart failure in such individuals. Development of such diastolic heart failure is accompanied by progressive accumulation of extracellular matrix in the absence of left ventricular dilation (Mandinov et al., 2000; Nishikawa et al., 2003), and the most common underlying condition is hypertensive heart disease (Vasan et al., 1999).

Nifedipine, a dihydropyridine-based Ca^{2+} antagonist, is widely used for the treatment of hypertension. This drug is thought to reduce blood pressure and increase coronary blood flow by specifically inhibiting the entry of Ca^{2+} into smooth muscle cells through L-type Ca^{2+} channels (Saida and van Breemen, 1983). Nifedipine also exerts effects in cultured endothelial cells, however, even though these cells do not express L-type Ca^{2+} channels (Fukuo et al., 2002). Nifedipine has been shown to promote re-endothelialization after vascular injury, and it is thought to protect against atherosclerosis through inhibition of endothelial cell apoptosis and suppression of vascular inflammation, effects that have been attributed to antioxidant properties of the drug (Fukuo et al., 2002; Sugano et al., 2002). However, little is known of the possible effects of nifedipine on the myocardium.

The ACTION (A Coronary disease Trial Investigating Outcome with Nifedipine GITS) trial showed that treatment with long-acting

* Corresponding author. Tel./fax: +81 52 719 1546.
E-mail address: nagata@met.nagoya-u.ac.jp (K. Nagata).

0014-2999/$ – see front matter © 2009 Elsevier B.V. All rights reserved.
doi:10.1016/j.ejphar.2009.05.028